Supporting Information

Zinc(II) Complex of Di(naphthylethynyl)azadipyrromethene with low synthetic complexity leads to OPV with high industrial accessibility

Chunlai Wang,[1] Peiran Wei,[1] Jenner H.L. Ngai,[2] Arnold L. Rheingold,[3] Thomas G. Gray,[1] Yuning Li,[2] Emily Pentzer,[1] Ruipeng Li,[4] Lei Zhu,[5] and Geneviève Sauvé [1,*]

[1] Department of Chemistry, Case Western Reserve University, Cleveland, Ohio 44106-7078, United States

[2] Department of Chemical Engineering and Waterloo Institute for Nanotechnology (WIN) University of Waterloo, Waterloo, Ontario, Canada, N2L 3G1

[3] Department of Chemistry and Biochemistry, University of California, San Diego, La Jolla, California 92093, United States

[4] National Synchrotron Light Source II, Brookhaven National Laboratory, Upon, New York 11973, United States

[5] Department of Macromolecular Science and Engineering, Case Western Reserve University, Cleveland, Ohio 44106-7202, United States

* Corresponding author, E-mail: gxs244@case.edu (G.S.).

Experimental

Materials. 4-hexylacetophenone (Aldrich), benzaldehyde (Aldrich), *n*-butyllithium solution (Aldrich), tributyltin chloride (Fisher), tributyl(phenylethynyl)tin (Aldrich), tetrakis(triphenylphosphine)palladium(0) (Aldrich), bis(triphenylphosphine)platinum(II) chloride (Aldrich), copper(I) iodide (TCI America), *n*-iodosuccinimide, (abbreviated as NIS, Aldrich), anhydrous *o*-dichlorobenzene (abbreviated as *o*-DCB, Aldrich), nitromethane (Aldrich), ferrocene (Aldrich), diethylamine, anhydrous dichloromethane (Aldrich), zinc chloride (Aldrich), trimethylamine (Aldrich), acetic acid ((Fisher), chloroform (Aldrich) and 1-ethynylnaphthalene (TCI America) were used as received. Xylenes and tetrahydrofuran (THF) were distilled over sodium and stored in a refrigerator before use. All other chemicals were purchased from either Sigma Aldrich or Fisher Scientific, and used as received.

General Characterization Methods and Instrumentation. Proton nuclear magnetic resonance (^{1}H NMR) spectra were recorded using a 500 MHz Bruker Ascend Advance III High Definition (HD). Chemical shifts were reported in parts per million (ppm) relative to tetramethylsilane, $Si(CH_3)_4$. Matrix-assisted laser desorption/ionization time-of-flight (MALDI-TOF) mass spectra (MS) were measured on a Bruker Autoflex III MALDI-TOF mass spectrometer, and samples were prepared from chloroform solutions using a terthiophene matrix. Elemental analyses (C, H, N and Zn) were performed under optimum combustion conditions by Robertson Microlit Laboratories (Ledgewood, NJ).

UV-Vis absorption spectra were collected on a Cary 50 UV-Vis spectrometer. All solutions were made using chloroform with concentrations range from 3 mg/L to 9 mg/L. Molar absorptivities were obtained by extracting the slopes from plotting of relationships between absorbances and molar concentrations. All films were prepared from a 10 mg/mL solution in

chloroform. The solution was filtered through a 0.45 μm PTFE filter, then spin-coated at 800 rpm for 60 s. All films were annealed at 120 °C for 15 min before measurement.

Cyclic voltammetry (CV) measurements were performed at room temperature using an Autolab PGSTAT 302N Exo Chemie potentiostat. CV measurements were carried out using 0.1 M Bu$_4$NPF$_6$ in dry dichloromethane (DCM) as the electrolyte solution and ferrocene/ferrocenium as the internal standard. The solution was purged with nitrogen for 5 min prior to the measurement. A polished glassy carbon (GC) electrode served as the working electrode and two Pt wires were used as the counter and pseudo-reference electrodes. 5 mg zinc(II) complexes were fully dissolve in the electrolyte solution before measurement. All scans were performed at a scan rate of 0.1 V/s. The highest occupied molecular orbital (HOMO) energy levels and lowest occupied molecular orbital (LUMO) energy levels were estimated from the reversible half-peak potential (E$_{1/2}$) values in dichloromethane solution, using the value of -5.1 eV for Fc/Fc$^+$, i.e., HOMO = -(E$_{1/2\ ox}$ + 5.1) eV.

Thermal gravimetric analysis (TGA) was performed on a TA instrument Q500 thermogravimetric analyzer. Weight loss was recorded by heating the sample from 25 to 800 °C at a heating scan rate of 20 °C/min. DSC was performed on a TA Instruments Q2000 differential scanning calorimeter with a scanning rate of 10 °C/min up to 310 °C.

Crystals of Zn(L1)$_2$ and Zn(L2)$_2$ were obtained by the slow evaporation of dichloromethane from an acetonitrile solution. The crystals of Zn(L1)$_2$ and Zn(L2)$_2$ were diamond shaped and were dark purple in appearance. Multiple methods were attempted to crystallize Zn(WS3)$_2$, such as slow evaporation of dichloromethane from an acetonitrile solution and slow diffusion of pentane into a dichlorobenzene solution. However, we could only obtain very small needle-shaped crystals of Zn(WS3)$_2$ that diffracted very weakly and only to about 1.4 Å, due to

the small size of the Zn(WS3)$_2$ crystals. Crystallographic data (excluding structure factors) for the structure(s) reported in this paper have been deposited with the Cambridge Crystallographic Data Centre (CCDC). The CCDC numbers for Zn(L1)$_2$ and Zn(L2)$_2$ are 1916509 and 1916510, respectively. Single-crystal X-ray diffraction studies were carried out using a Rigaku Rapid II diffractometer using Cu Kα (λ = 1.54178 Å) radiation monochromated using laterally graded multilayer (Goebel) mirror focusing optics. A single crystal was mounted on a Mitegen loop and cooled to 100 K for data collection. Unit cell parameters were measured and data were collected using the Rigaku CrystalClear software. Data were reindexed and integrated using HKL3000, scaled, and corrected for absorption using Scalepack.[1] The space group was assigned and the structure was solved by direct methods using the SHELXTL suite of programs and refined by full matrix least squares against $F2$ with all reflections using Shelxl 2014 and graphical interface Shelxle.[2-4] H atoms attached to carbon atoms were positioned geometrically and constrained to ride on their parent atoms, with carbon hydrogen bond distances of 0.95 Å for aromatic C–H and 0.99 Å for alkane moieties, respectively. Uiso(H) values were set to 1.2 times Ueq(C).

For DTF calculations, spin-restricted density-functional calculations were performed in Gaussian16 rev. A.03.[5] Geometries were fully optimized in the gas-phase using the 6-31G(d) basis set[6] on all atoms. Harmonic vibrational frequency calculations found all real frequencies, confirming the converged structures to be local minima of the potential energy hypersurfaces. Calculations employed Becke's three-parameter hybrid exchange functional and the correlation functional of Lee, Yang, and Parr.[7-10] Franck-Condon singlet excited states were calculated on gas-phase 6-31G(d) geometries of the respective ground states with the TZVP basis set[11] for all atoms. Continuum solvation in chloroform was included using the integral equation formalism of

the polarizable continuum model.[12-15] Population analyses were performed with the AOMix program of Gorelsky.[16, 17]

For single-carrier device fabrication, ITO-coated glass substrates were cleaned stepwise in soapy water, DI water, acetone and isopropanol under ultrasonication for 15 minutes followed to a Reactive Ion Etcher (RIE) treatment for 30 seconds. Hole-only devices had the device structure: ITO/PEDOT:PSS/active layer/MoO_3/Ag. The PEDOT:PSS layer was prepared by filtering a water solution of 1.3 wt % PEDOT:PSS through a 0.45μm PTFE filter followed by spin coating at 4000 rpm for 60 seconds and heated at 150 °C for 10 minutes. The photoactive layers were spin coated inside the glovebox at 1000 rpm for 40 seconds followed by 2000 rpm for 2 seconds from a blend solution with a total concentration of 20 mg/mL in o-DCB. The solutions were filtered through a 0.45μm PTFE filter prior to spin coating. $Zn(L1)_2$ and $Zn(L2)_2$ were blended with P3HT in 1:0.8 and 1:1.3 ratio, respectively. All active layers were deposited from o-DCB solutions. The active layer thicknesses were about 80 nm. The photoactive layers were annealed either at 80°C for 15 min for neat films, 100°C for 15 min for P3HT:$Zn(L1)_2$ films or 120°C for 15 min for P3HT:$Zn(L2)_2$ films. This was followed by thermal deposition of MoO_3 (10 nm) and Ag (80 nm) using the Angstrom Engineering Evovac Deposition System. For electron-only devices with an ITO/ZnO/active layer/Ca/Al structure, cleaning of the ITO substrate, ZnO film and active layer film formation was performed as previously described. Calcium (30 nm) and Al (100 nm) were thermally deposited. Dark current measurements were performed using a Keithley 2400 source meter inside the glovebox. The devices have a total effective area of 0.20 cm².

For organic photovoltaic (OPV) device fabrication, the inverted structure (ITO/ZnO/P3HT:acceptor/MoO_3/Ag) was used for all devices. ITO-coated glass substrates cleaning, ZnO layer, MoO_3 layer, and Ag layer were prepared by the same procedure mentioned

in the charge-carrier device fabrication. For P3HT:zinc(II) complexes devices, active layers were prepared from varied weight ratios of P3HT: acceptor with varied concentration in o-DCB solution by spin coating at 1000 rpm for 40 seconds and followed by 2000 rpm for 2 seconds. The optimized conditions for P3HT:PCBM, P3HT:Zn(L1)$_2$ and P3HT:Zn(L1)$_2$ were listed in Figure S8. For Zn(L2)$_2$:P(NDI2OD-T2) devices, the active layer was prepared from a 1:1 weight ratio of Zn(L2)$_2$:P(NDI2OD-T2) with 25 mg/mL concentration in o-DCB by using the same spin coating conditions as P3HT devices. All solutions were filtered through 0.45μm PTFE filters prior to spin coating. The photoactive layers were annealed at different temperatures before MoO$_3$ deposition. The optimized annealing conditions for P3HT:PCBM, P3HT:Zn(L1)$_2$ and P3HT:Zn(L1)$_2$ were. 120°C for 30 min, 100°C for 15 min and 120°C for 15 min, respectively. For the Zn(L2)$_2$:P(NDI2OD-T2) system, the film was annealed at 80°C for 15 min. The devices have a total effective area of 0.20 cm².

OPV measurements were done inside the glovebox (Pure LabHE) under 1.5 AM solar illumination at intensity of 100 mW/cm² using Oriel Sol2A solar simulator and Keithley 2400 IV station. The light intensity dependence of J-V characterisitics were measured under simulated illumination at varied power intensity. Light intensity was calibrated by using a standard silicon solar cell in the glovebox. Incident Photon-to-Charge Carrier Efficiency was measured in air on fabricated OPV devices using a QEX10 Quantum Efficiency Measurement System. To minimize potential degradation in air, the devices were measured immediately after taking them out of the glove-box.

The thin-film-transistors (TFTs) were fabricated as bottom-gate-bottom-contact (BGBC) geometry devices. Electrode pattern was made by using photolithography techniques in a cleanroom facility. Gold was used as the source/drain electrodes and the dimension of the

electrodes are 30 microns for channel length and 1000 microns for channel width. For the fabrication procedures, the n-doped Si substrates with a 300 nanometer-thick SiO_2 as the dielectric layer were sonicated in chloroform, acetone and alcohols, and then the surface was cleaned by plasma treatment. The Si/SiO_2 substrate surface was modified by a dodecyltrichlorosilane (or DDTS) solution (10 mM in toluene) by submerging the substrate in the solution for 20 minutes to deposit a self-assembled monolayer on the SiO_2 surface. The zinc(II) complex solutions were prepared as 10 mg/mL in o-DCB and spin coated on the Si/SiO_2 substrates at 3000 rpm for 60 seconds. The zinc(II) complex film thicknesses were around 40 nanometers. Films were fabricated and characterized using Agilent B2912A Semiconductor Analyser in an argon-filled glovebox at room temperature. The mobility in the saturation region was calculated using the following equation:

$$I_{DS} = \left(\frac{WC_i}{2L}\right)\mu(V_G - V_T)^2$$

where I_{DS} is the source-drain current, μ is the charge carrier mobility, C_i is the capacitance per unit area of the dielectric (11.6 nF cm^{-2} for DDTS modified SiO_2), W (1000 microns) and L (30 microns) are TFT channel width and length, V_G is the gate voltage, and V_T is the threshold voltage.

Tapping-mode atomic force microscopy (AFM) was performed on blend films using a Park NX 10 Atomic Force Microscope (XEP 3.0.4 Build 37). The acquired images were processed and analyzed using XEI (1.8.0, Build 36).

Grazing incidence wide angle X-ray diffraction (GI-WAXD) sample preparation: the silicon wafers were sonicated in deionized water, acetone and isopropanol, followed by oxygen plasma etching to clean the surface of silicon oxide. ZnO films were prepared on the top of SiO_2 by using the same procedure as in the OPV fabrication. All active layers were spin-coated on top of ZnO layer from a concentration of 25 mg/mL in o-DCB solution. The spin-coating condition is

same as the OPV active layer fabrication conditions. The thickness of samples was around 100 nm. All samples were prepared as two sets: annealed and as-cast. Annealing conditions were the same as the OPV fabrication conditions: 100°C for 15 min for $Zn(L1)_2$ based films and 120°C for 15 min for $Zn(L2)_2$- based films. GI-WAXD measurements were performed using the 11-BM Complex Materials Scattering (CMS) beamline at the National Synchrotron Light Source II (NSLS-II), Brookhaven National Laboratory. The monochromatized X-ray wavelength was $\lambda =$ 0.0918 nm. An in-vacuum CCD detector (Photonic Science) was used to collect GI-WAXD patterns. The polymer films were illuminated by the collimated X-ray beam at an incidence angle of about 0.1°. The distance between the sample and the detector was 222.2 mm, which was calibrated using silver behenate with the first-order reflection at a scattering vector of $q = 1.076$ nm^{-1}. The data acquisition time for each GI-WAXD pattern was 10 s. Polar (Stony Brook Technology and Applied Research, Inc., Stony Brook, NY) software was used for data analysis. Fraser correction was performed for all 2D GI-WAXS patterns.

Synthesis

Tributyl(naphthalenyl-1-ethynyl)tin (a). 1-ethynylnaphthalene (2 g, 13.2 mmol) and 15 mL dry THF were added into a pre-dried 50 mL three-neck round-bottom flask under nitrogen and the mixture was cooled to -78 °C by using an acetone-dry ice bath. 5.2 mL n-butyllithium solution (2.5 M in hexane) was added into the reaction dropwise. After stirring for 1 h at -78 °C, tributyltin chloride (4.2 g, 13.2 mmol) was added dropwise and the mixture was stirred at 25 °C for 1 h. THF and hexane in the mixture were evaporated by using rotary evaporation to obtain a yellow liquid, followed by vacuum filtration through a filter paper. The residue on top of the filter paper was washed with 50 mL hexane and all filtrates were collected and evaporated under vacuum to obtain a light yellow oily product (5.7 g, 13.1 mmol, 99% yield). ^{1}H NMR (500 MHz, $CDCl_3$, δ): 7.93

(s, 1H), 7.80-7.67 (m, 3H), 7.51-7.39 (m, 3H), 1.65-1.57 (m, 6H), 1.35 (dt, J = 14.7, 7.4 Hz, 6H), 1.08-1.03 (m, 6H), 0.9 (t, J = 7.3 Hz, 9H).

4-hexylchalcone. 4-hexylacetophenone (8.7 g, 43 mmol), benzaldehyde (5 g, 47 mmol), and 70 mL methanol were added into a 250 mL one-neck round-bottom flask and the mixture were stirred at 25 °C. 25 mL 5 M sodium hydroxide solution was added into the flask dropwise and the reaction was stirred at 25 °C for 24 h. The reaction was poured into 200 mL cold water to precipitate the product and then vacuum filtered through a filter paper to collect a light yellow solid product (11 g, 38 mmol, 88% yield). ^{1}H NMR (500 MHz, CDCl₃, δ): 7.96 (d, J = 8.1 Hz, 2H), 7.81 (d, J = 15.7 Hz, 1H), 7.65 (dd, J = 6.5, 2.8 Hz, 2H), 7.55 (d, J = 15.7 Hz, 1H), 7.45-7.39 (m, 3H), 7.31 (d, J = 8.2 Hz, 2H), 2.68 (dd, J = 14.7, 6.9 Hz, 2H), 1.65 (dt, J = 15.3, 7.6 Hz, 2H), 1.39-1.26 (m, 6H), 0.89 (t, J = 6.9 Hz, 3H).

***pr*-hexylADP.** *pr* represents proximal phenyl substitution on ADP. 4-hexylchalcone (8 g, 27 mmol), diethylamine (abbreviated as DEA, 10 g, 137 mmol), nitromethane (8.35 g, 137 mmol) and 80 mL methanol were added into a 250 mL one-neck round-bottom flask and the mixture was stirred and refluxed for 24 h. Solvent, DEA and nitromethane were evaporated to obtain nitro-4-hexylchalcone as brownish oily crude product 8.4 g (24 mmol, 87% yield). The crude product was added into a 500 mL one-necked round-bottom flask with ammonium acetate (60 g, 78 mmol) and 270 mL butanol and the reaction was stirred and refluxed for 24 h. The reaction was cooled down to 0 °C to precipitate the product and the mixture was vacuum filtered through a filter paper. After washing the solid with methanol, a dark blue product was obtained (11 g, 18 mmol, 65% yield). ^{1}H NMR (500 MHz, CDCl₃, δ): 12.17 (s, 1H), 8.07 (d, J = 7.3 Hz, 4H), 7.87 (d, J = 8.1 Hz, 4H), 7.42 (d, J = 7.5 Hz, 4H), 7.38-7.32 (m, 6H), 7.18 (s, 2H), 2.70 (t, J = 7.7 Hz, 4H), 1.73-1.65 (m, 4H), 1.44-1.31 (m, 12H), 0.91 (t, J = 7.0 Hz, 6H).

***pr*-hexylADPI₂.** pr-hexylADP (5 g, 8 mmol), NIS (4.6 g, 20 mmol), 15 mL acetic acid and 500 mL chloroform were added into a 1 L one-neck round-bottom flask and the mixture was stirred at 25 °C for 5 h under dark. The solvents were evaporated by using rotary evaporation to obtain dark blue solid. After washing the solid with methanol, the product was obtained as a dark blue solid (7.8 g, 9 mmol, 95% yield). ^{1}H NMR (500 MHz, CDCl₃, δ): 12.24 (s, 1H), 7.91 (d, J = 8.1 Hz, 4H), 7.74-7.67 (m, 4H), 7.39-7.31 (m, 10H), 7.38-7.32 (m, 6H), 2.70 (t, J = 7.7 Hz, 4H), 1.68 (dt, J = 15.4, 7.5 Hz, 4H), 1.44-1.31 (m, 12H), 0.91 (t, J = 7.0 Hz, 6H).

L1. *pr*-hexylADPI₂ (0.5 g, 0.58 mmol), tributyl(phenylethynyl)tin (0.8 g, 2 mmol), Pd(PPh₃)₄ (66 mg, 0.058 mmol) and 60 mL dry xylenes were added into a pre-dried 250 mL 3-neck round-bottom flask under nitrogen and the mixture was stirred at 125 ºC for 8 h. After cooling to 25 ºC, solvents were evaporated by rotary evaporation and 50 mL of methanol was poured into the mixture to precipitate the product. The precipitate was filtered through a filter paper and washed with 200 mLs of methanol to obtain a dark blue solid (0.42 g , 0.51 mmol, 89% yield). ^{1}H NMR (500 MHz, CDCl₃, δ): 12.54 (s, 1H), 8.27 (d, J = 8.2 Hz, 4H), 8.19 (d, J = 7.2 Hz, 4H), 7.49 (dd, J = 7.8, 1.4 Hz, 4H), 7.44 (t, J = 7.4 Hz, 4H), 7.41-7.32 (m, 12H), 2.72 (t, J = 7.7 Hz, 4H), 1.71 (dt, J = 15.4, 7.5 Hz, 4H), 1.44-1.31 (m, 12H), 0.92 (t, J = 6.9 Hz, 6H).

L2. *pr*-hexylADPI₂ (1.54 g, 1.79 mmol), tributyl(naphthalenyl-1-ethynyl)tin (**a**) (2.7 g, 6.2 mmol), Pd(PPh₃)₄ (203 mg, 0.179 mmol) and 100 mL dry xylenes were added into a pre-dried 250 mL 3-neck round-bottom flask under nitrogen and the mixture was stirred at 125 ºC for 8 h. After cooling to 25 ºC, the solvent was evaporated by rotary evaporation and 50 mL methanol was poured into the mixture to precipitate the product. The precipitate was filtered through a filter paper and washed with 200 mLs of methanol to obtain a dark blue solid (1.5 g , 1.63 mmol, 91% yield). ^{1}H NMR (500 MHz, CDCl₃, δ): 12.70 (s, 1H), 8.29 (t, J = 8.2 Hz, 6H), 8.25-8.19 (m, 4H),

7.80 (dd, J = 15.9, 8.1 Hz, 4H), 7.65 (d, J = 6.9 Hz, 2H), 7.52-7.48 (m, 2H), 7.47-7.40 (m, 10H), 7.36 (d, J = 8.0 Hz, 4H), 2.76 (t, J = 7.7 Hz, 4H), 1.74 (dt, J = 15.2, 7.6 Hz, 4H), 1.49-1.36 (m, 12H), 0.94 (t, J = 6.7 Hz, 6H). MALDI–TOF m/z: calcd for $C_{68}H_{59}N_3$, 917.47; found, 917.31.

Zn(L1)$_2$. L1 (0.3 g, 0.37 mmol), sodium hydride (15 mg, 0.63 mmol) and 8 mL dry THF were added into a pre-dried 100 mL 3-neck round-bottom flask under nitrogen and the mixture was stirred at 25 ℃ for 4 h. 50 mL anhydrous dichloromethane was added into the reaction followed by the dropwise addition of $ZnCl_2$ solution, which was prepared by dissolving $ZnCl_2$ (60 mg, 0.44 mmol) powder into a 4 mL MeOH. The reaction was stirred at 25 ℃ for 12 h and the crude product was obtained by evaporating all solvents. The crude product was purified by chromatography dichloromethane and hexane mixture (25 vol.% dichloromethane) as the eluent, and the first fraction with blue color was collected. The pure product was obtained as a dark blue solid after evaporation of solvents (0.25 g , 0.18 mmol, 61 % yield). ^{1}H NMR (500 MHz, CDCl$_3$, δ): 8.05 (d, J = 3.5 Hz, 8H), 7.62 (d, J = 8.0 Hz, 8H), 7.45-7.41 (m, 12H), 7.37 (d, J = 6.5 Hz, 8H), 7.32-7.27 (m, 12H), 7.00 (d, J = 7.9 Hz, 8H), 2.30-2.38 (m, 8H), 1.41-1.32 (m, 8H), 1.27-1.10 (m, 24H), 0.84 (dd, J = 14.5, 7.2 Hz, 12H). ^{13}C NMR (500 MHz, CDCl$_3$, δ) was shown in Figure S9. MALDI–TOF m/z: calcd for $C_{120}H_{108}N_6Zn$, 1697.79; found, 1697.05. anal. calcd for: C, 84.80; H, 6.41; N, 4.94; Zn, 3.85; found: C, 84.65; H, 6.36; N, 4.85; Zn, 4.17.

Zn(L2)$_2$. L2 (1.5 g, 1.65 mmol), sodium hydride (30 mg, 2.1 mmol) and 20 mL dry THF were added into a pre-dried 500 mL 3-neck round-bottom flask under nitrogen and the mixture was stirred at 55 ℃ for 4 h. 100 mL anhydrous dichloromethane was added into the reaction followed by the dropwise addition of $ZnCl_2$ solution, which was prepared by dissolving $ZnCl_2$ (136 mg, 1 mmol) powder into a 4 mL MeOH. The reaction was stirred at 25 ℃ for 12 h. The crude product was obtained by evaporating all solvents and was purified by washing with large

amounts of methanol and 20 mL acetone. The solid residue was washed with 50 mL dichloromethane under vacuum filtration. The filtrates were collected and the dichloromethane was evaporated to yield the pure product as a dark blue solid (1.3 g , 0.62 mmol, 86 % yield). ^{1}H NMR (500 MHz, CDCl$_3$, δ): 8.26-8.17 (m, 12H), 7.84 (d, J = 8.1 Hz, 4H), 7.82-7.77 (m, 12H), 7.61 (d, J = 6.7 Hz, 4H), 7.56-7.48 (m, 16H), 7.46-7.40 (m, 8H), 7.13 (d, J = 7.9 Hz, 8H), 2.48-2.39 (m, 8H), 1.45 (dt, J = 15.6, 7.7 Hz, 8H), 1.20 (ddd, J = 33.4, 14.6, 7.7 Hz, 24H), 0.84 (t, J = 7.2 Hz, 12H). ^{13}C NMR (500 MHz, CDCl$_3$, δ) was shown in Figure S10. MALDI–TOF m/z: calcd for C$_{136}$H$_{116}$N$_6$Zn, 1896.86; found, 1896.98. anal. calcd for: C, 85.98; H, 6.15; N, 4.42; Zn, 3.44; found: C, 85.71 H, 6.13; N, 4.31; Zn, 3.30.

1. ^{1}H NMR Spectra

Tributyl(naphthalenyl-1-ethynyl)tin (a)
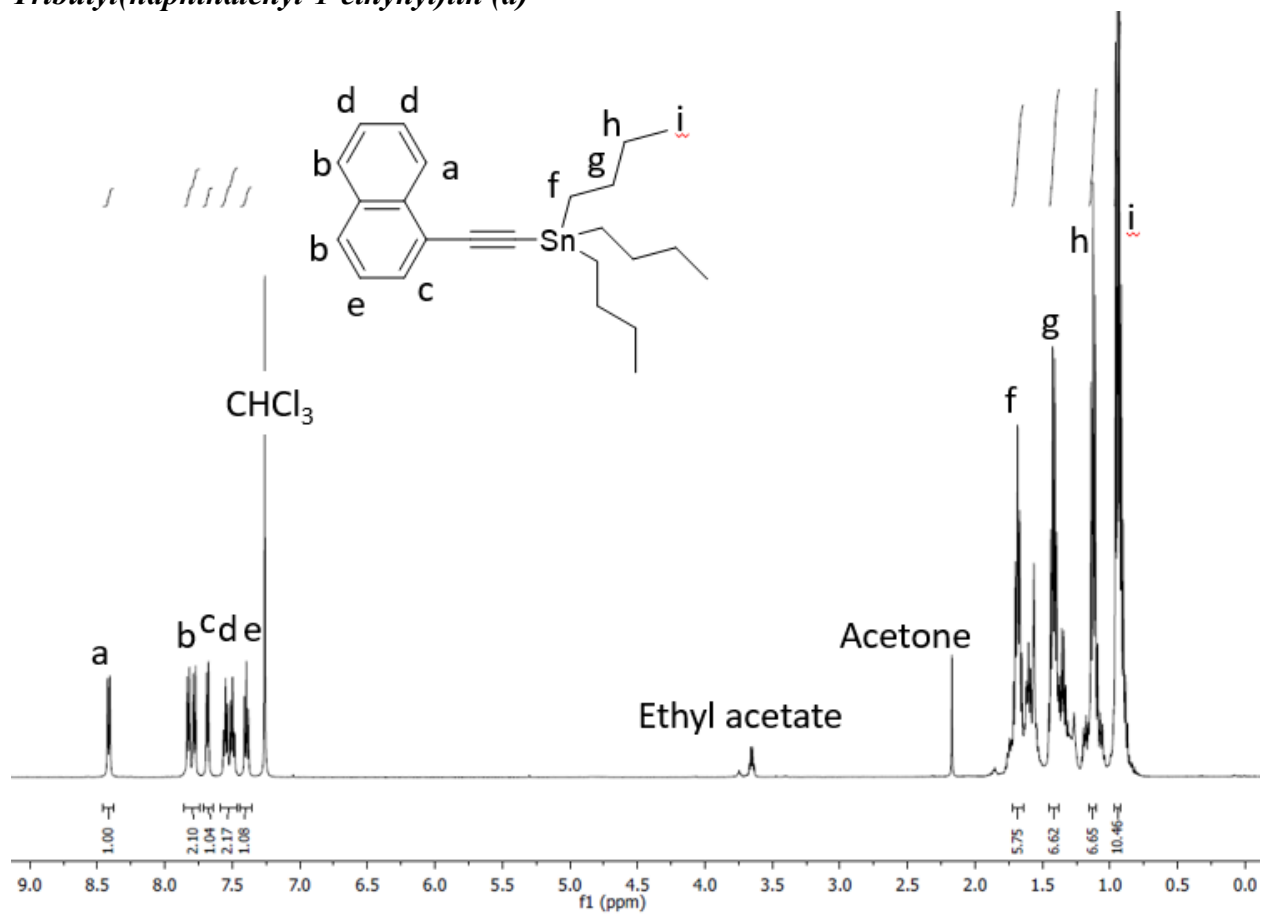
Figure S1. ^{1}H NMR spectrum of tributyl(naphthalenyl-1-ethynyl)tin (a). CDCl$_3$ was used as solvent. Residual acetone and ethyl acetate peaks are labelled.

4-hexylchalcone
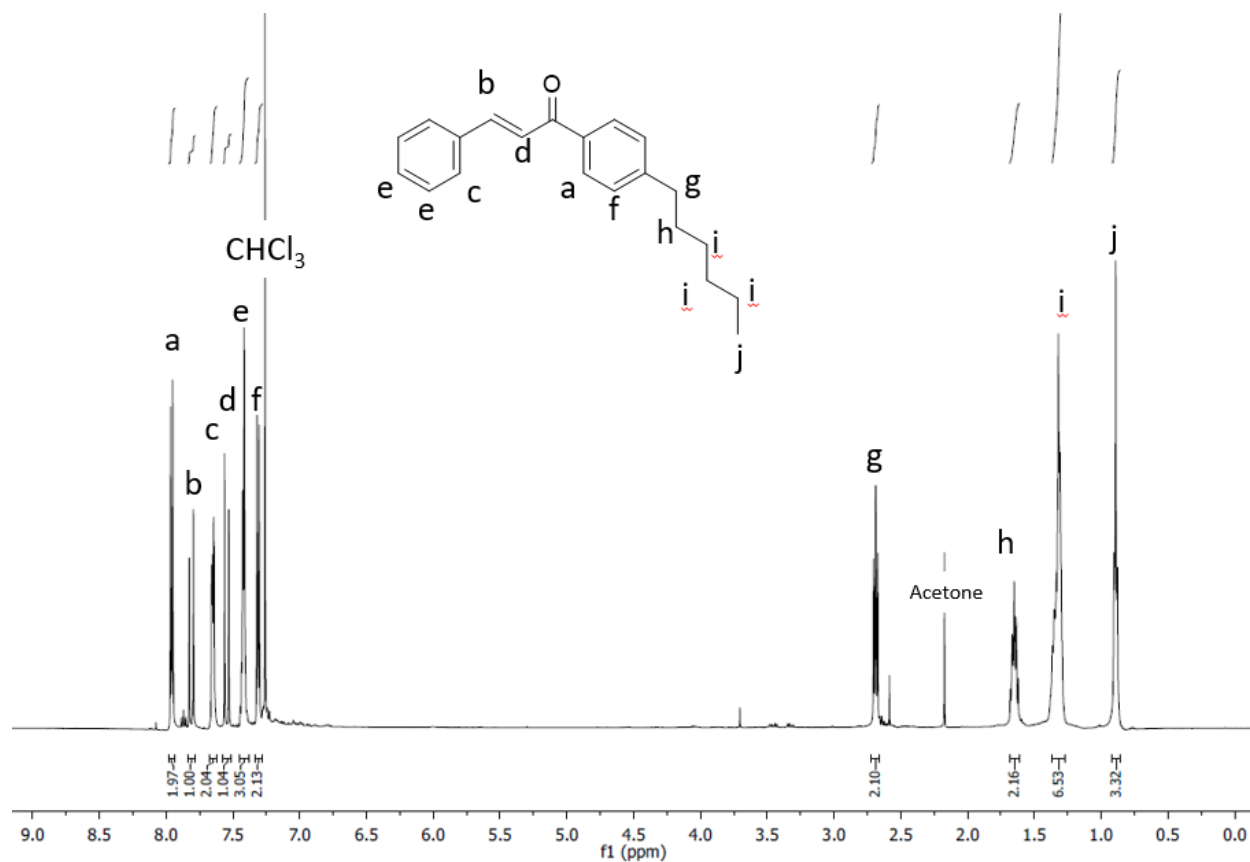
Figure S2. ^{1}H NMR spectrum of 4-hexylchalcone. CDCl$_3$ was used as solvent. Residual acetone peak is labelled.
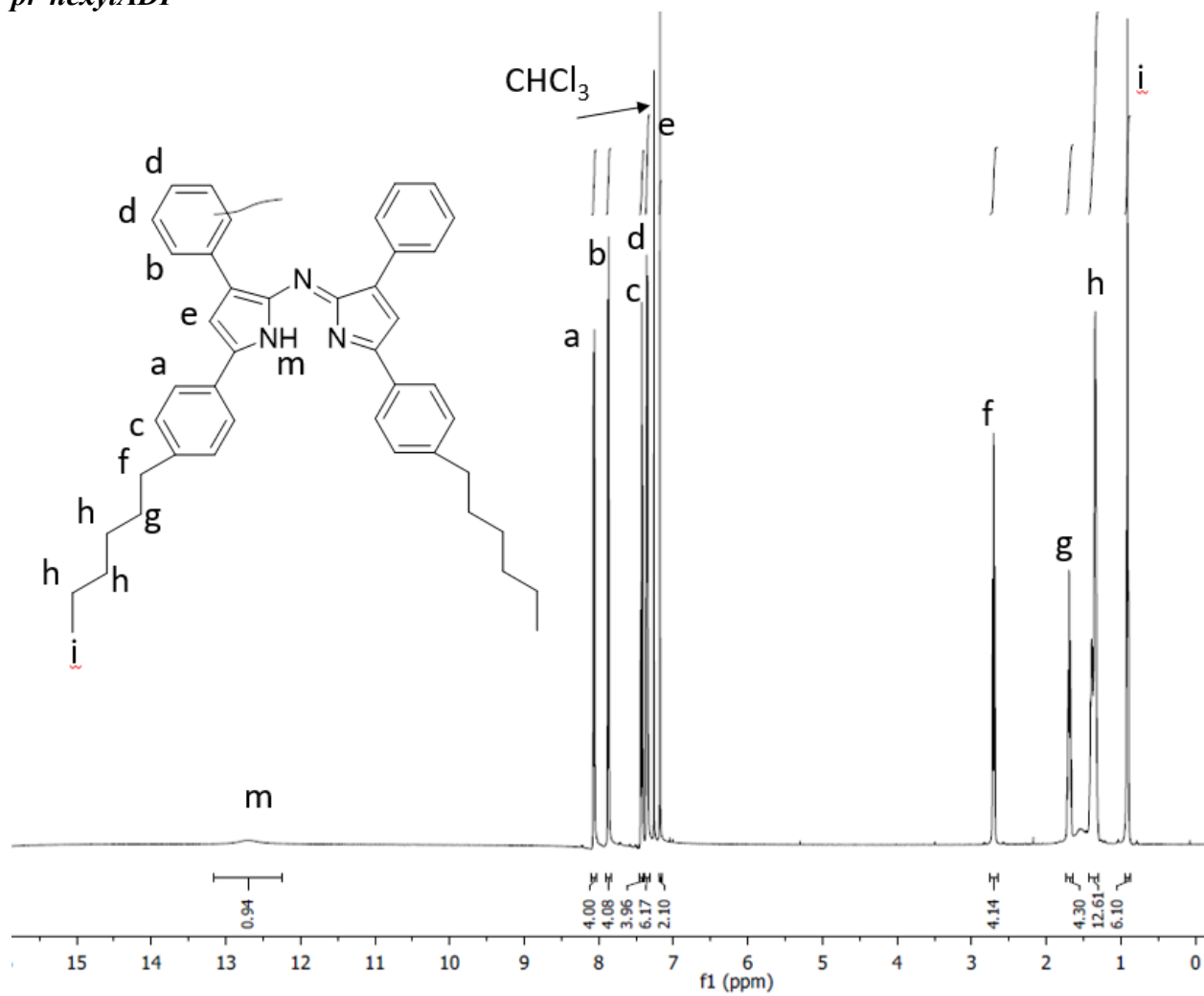
Figure S3. ^{1}H NMR spectrum of *pr*-hexylADP. CDCl$_3$ was used as solvent.

pr-hexylADPI₂
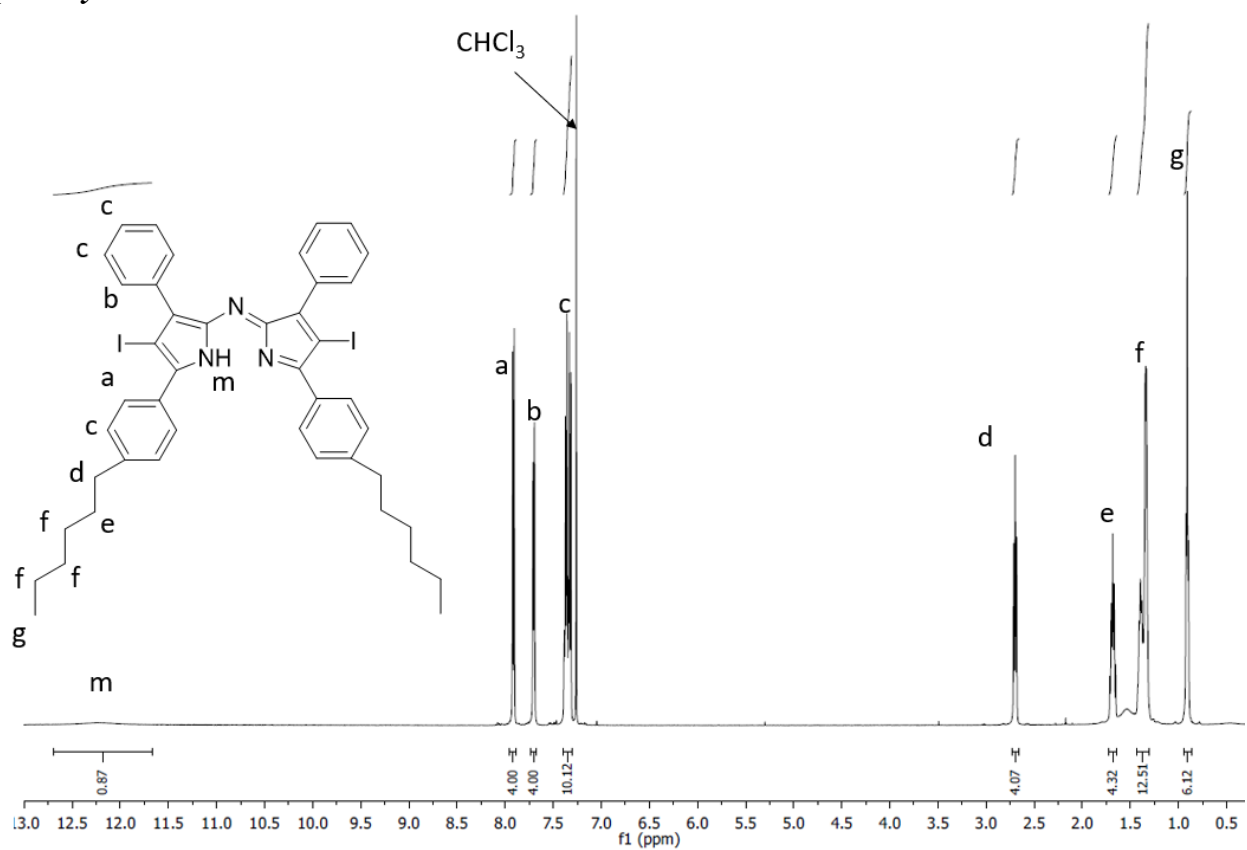
Figure S4. ¹H NMR spectrum of *pr*-hexylADPI₂. CDCl₃ was used as the solvent.

L1

Figure S5. ¹H NMR spectrum of L1. CDCl₃ was used as the solvent. Residual methanol peak is labelled, and water peak is seen at 1.56 ppm.
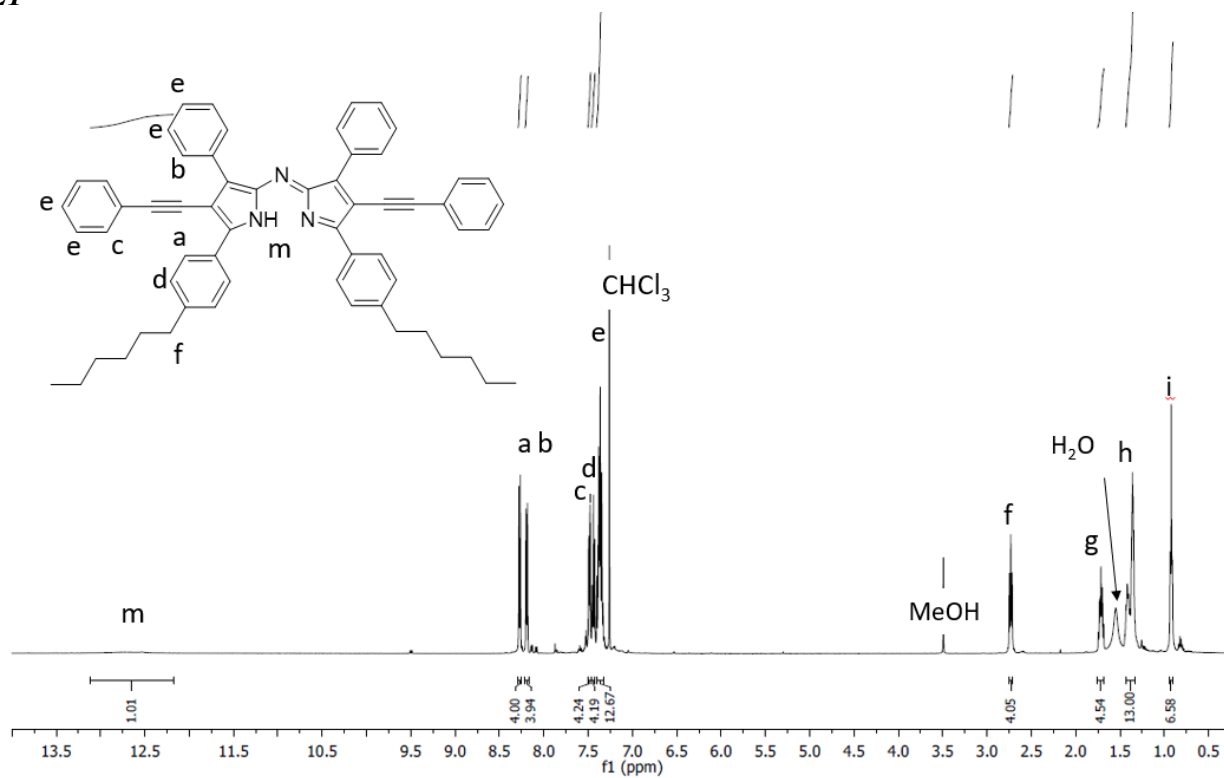
L2
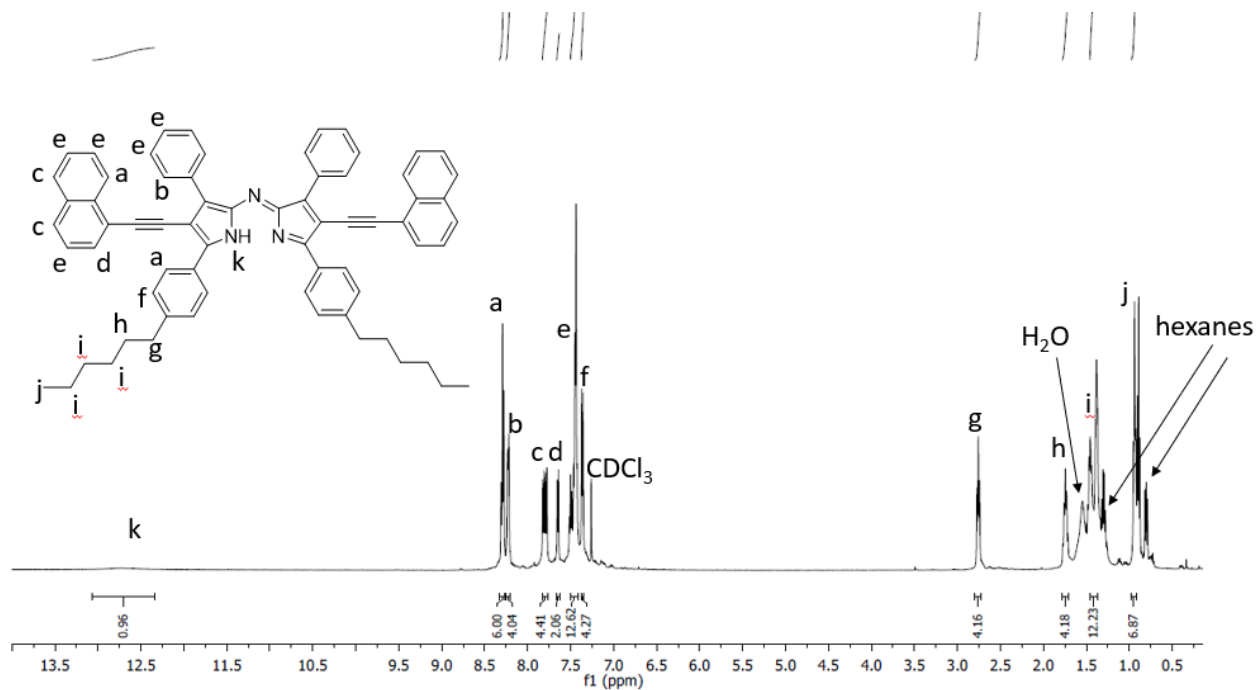
Figure S6. ^{1}H NMR spectrum of L2. CDCl$_3$ was used as the solvent. Residual hexane peak is labelled, and water peak is seen at 1.56 ppm.

Zn(L1)$_2$
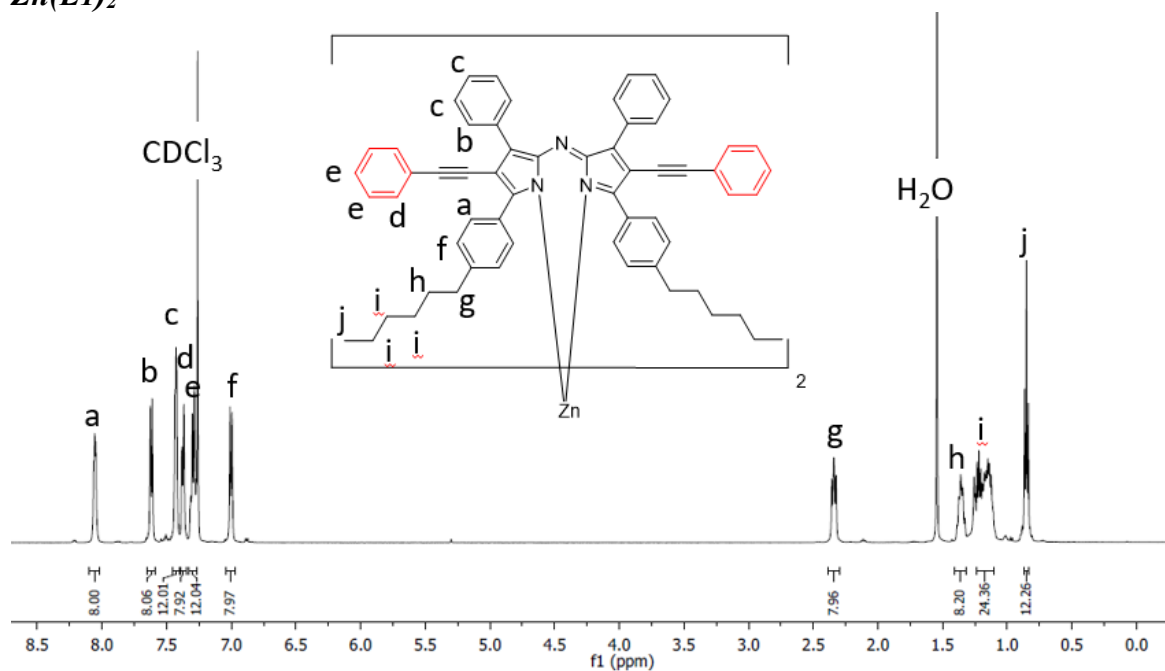
Figure S7. ^{1}H NMR spectrum of Zn(L2)$_2$. CDCl$_3$ was used as the solvent. Water peak is seen at 1.56 ppm.

Zn(L2)₂
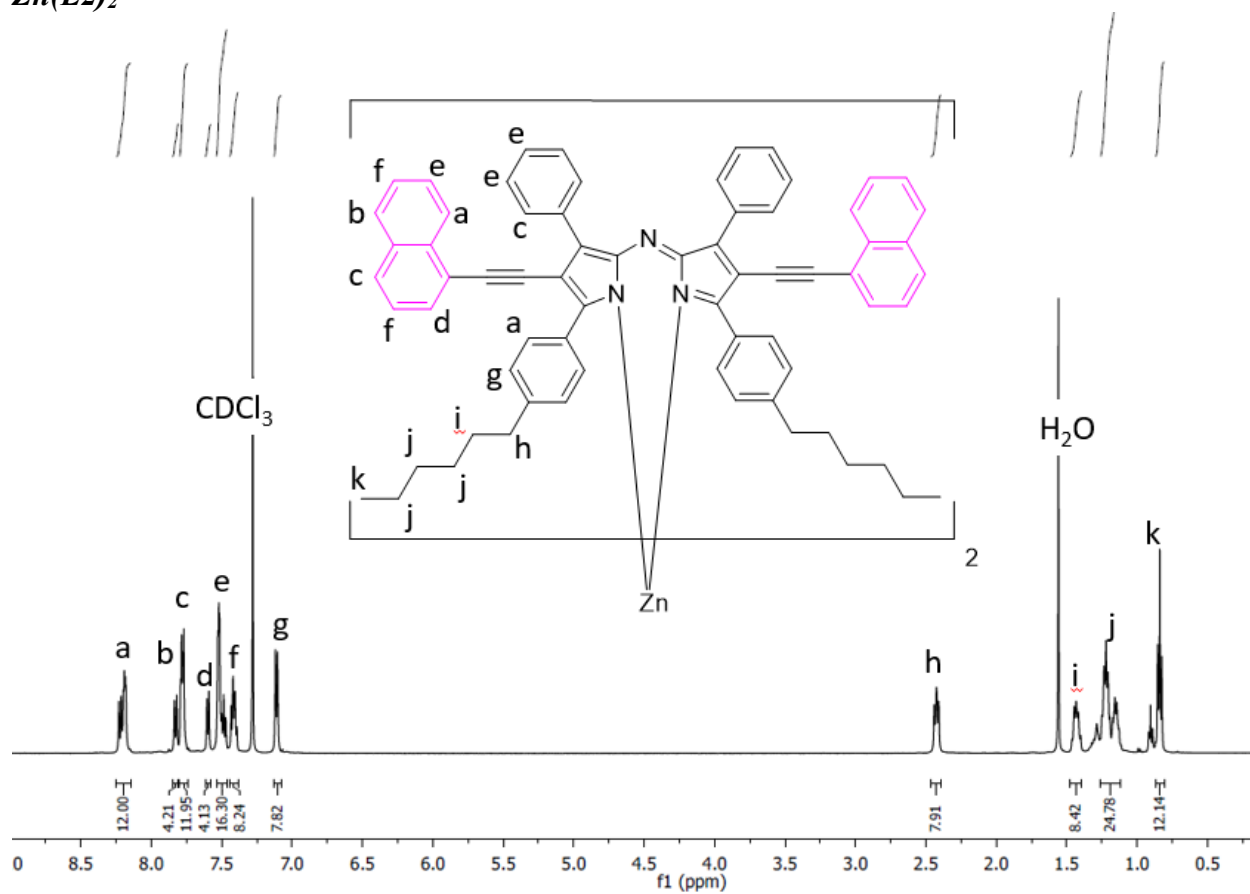
Figure S8. ¹H NMR spectrum of Zn(L2)₂. CDCl₃ was used as the solvent. Water peak is seen at 1.56 ppm.
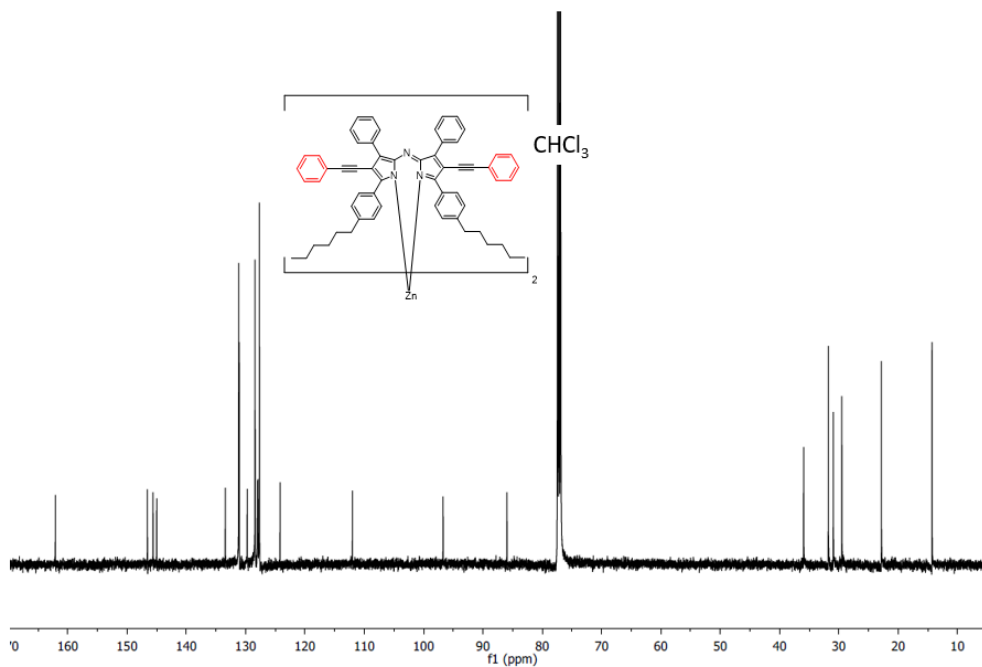
Figure S9. ^{13}C NMR spectrum of Zn(L1)$_2$. CDCl$_3$ was used as the solvent.
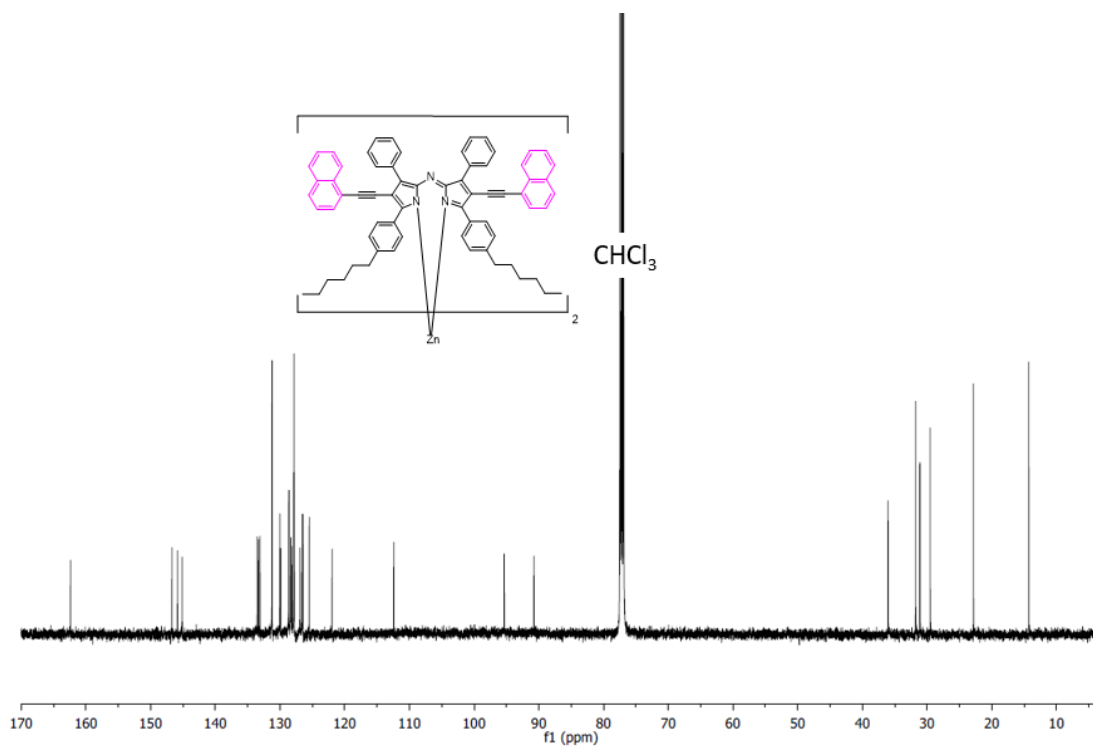
Figure S10. ^{13}C NMR spectrum of Zn(L2)$_2$. CDCl$_3$ was used as the solvent.

2. MALDI-TOF Mass Spectra
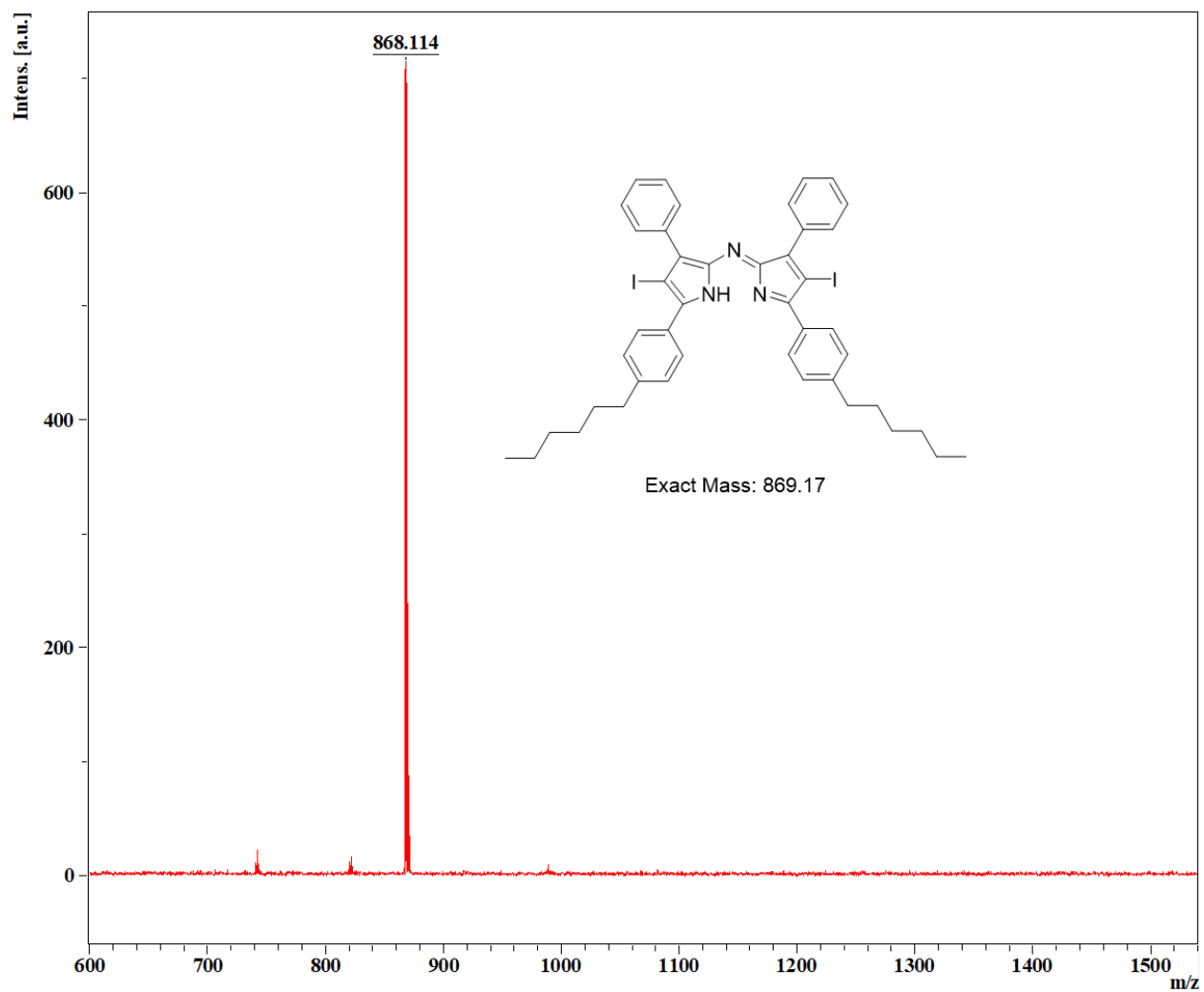
Figure S11. MALDI-TOF mass spectrum of *pr*-hexylADPI₂.

Exact Mass: 817.44
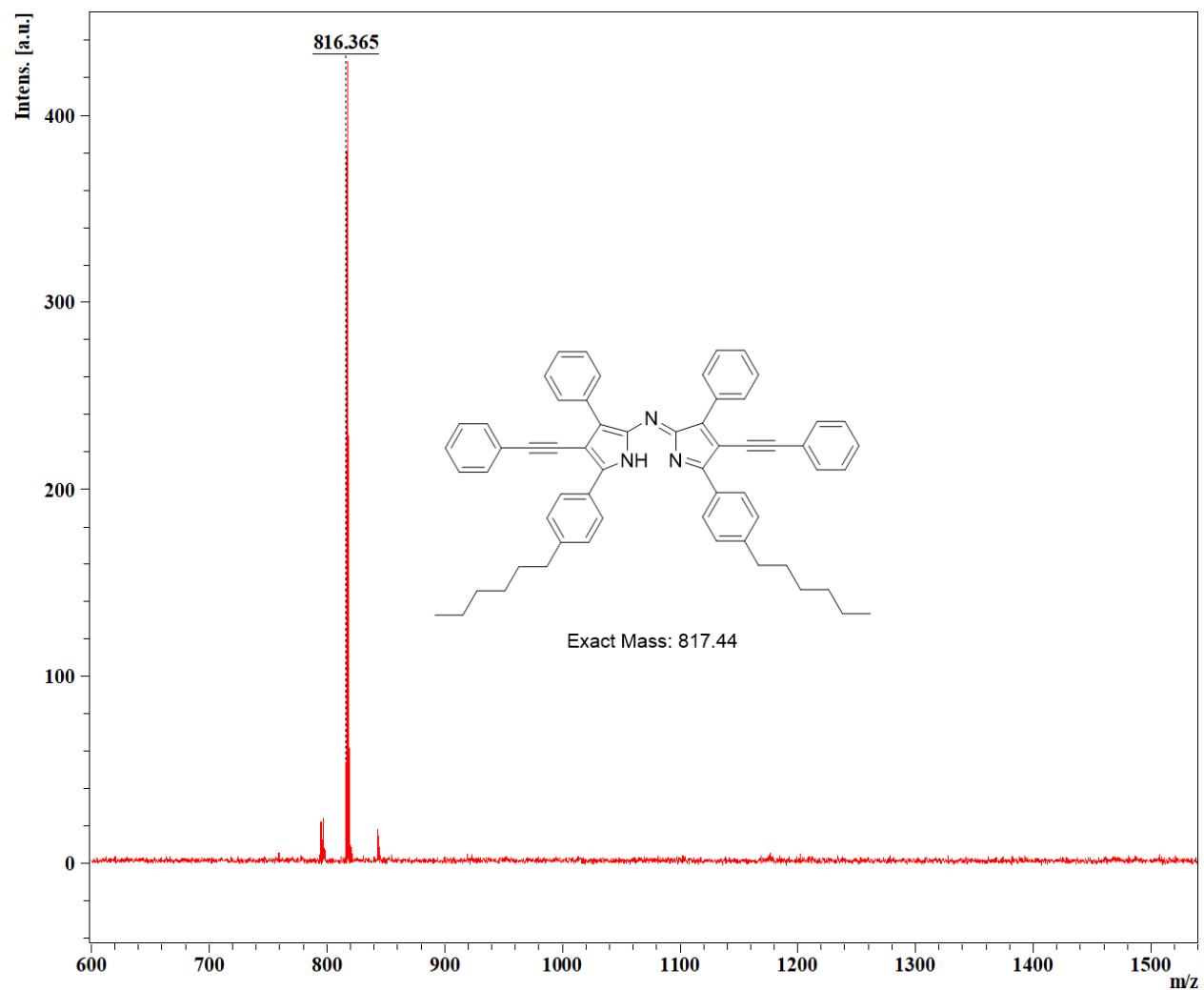
Figure S12. MALDI-TOF mass spectrum of L1.
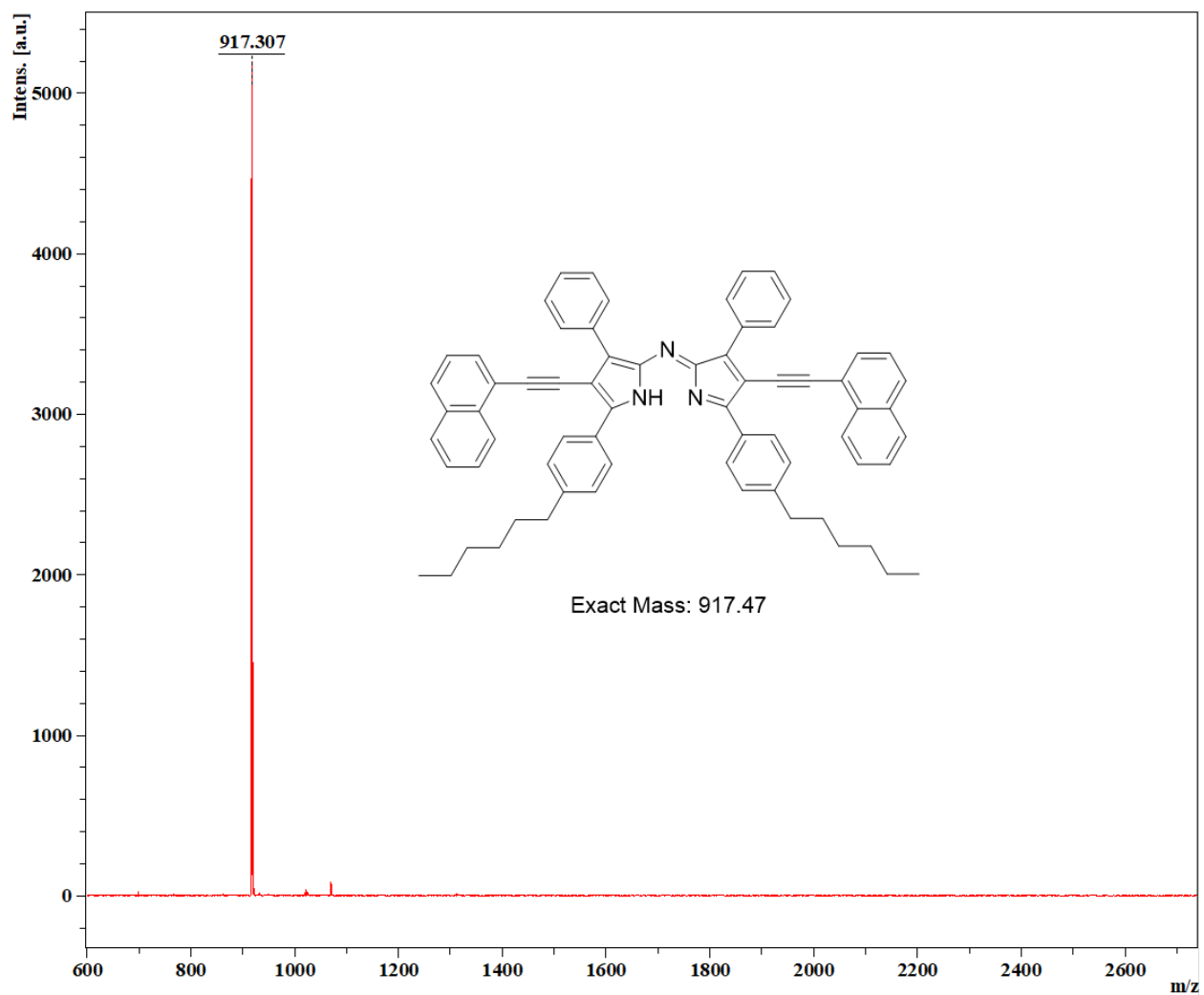
Figure S13. MALDI-TOF mass spectrum of L2.
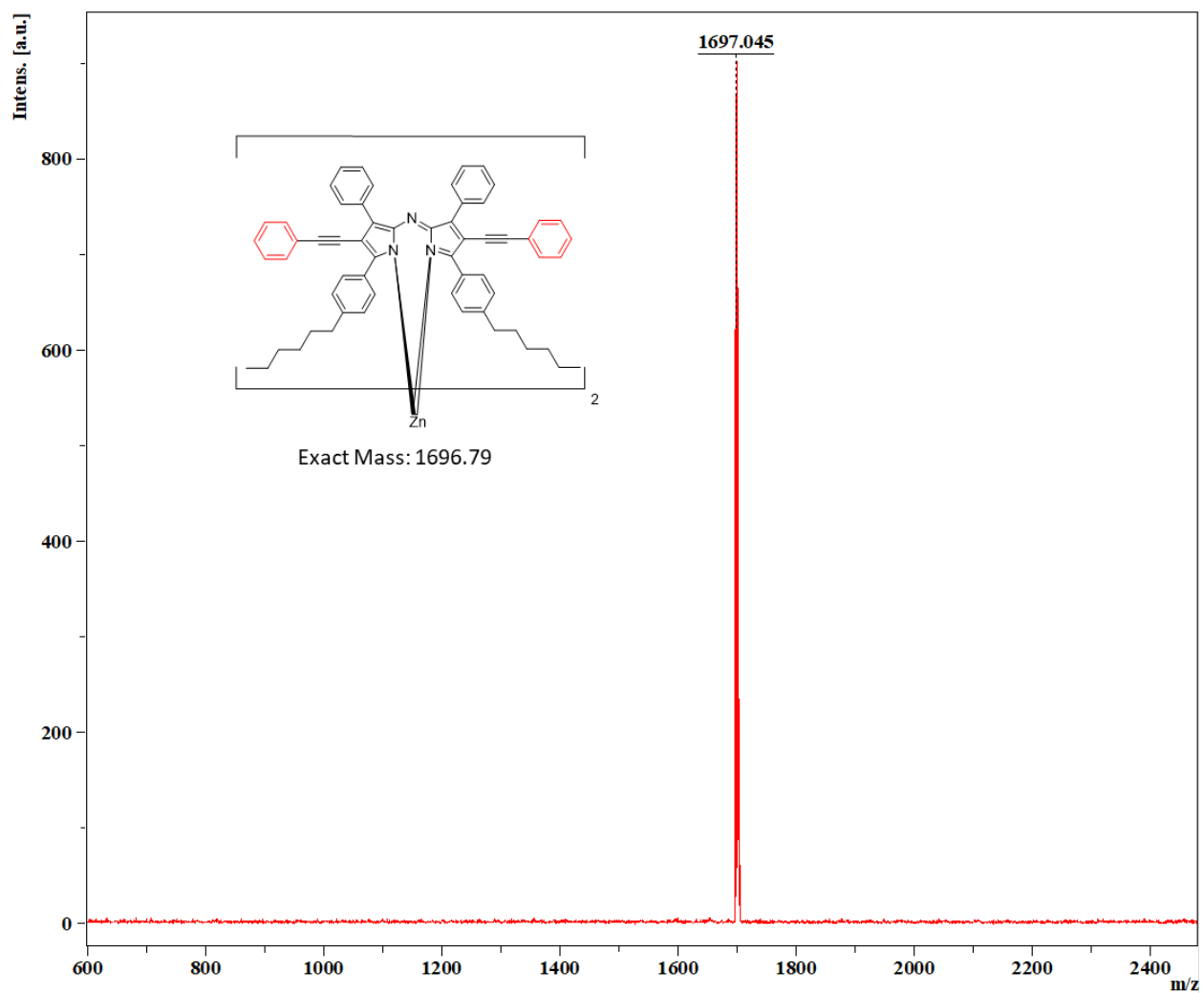
Figure S14. MALDI-TOF mass spectrum of Zn(L1)₂.
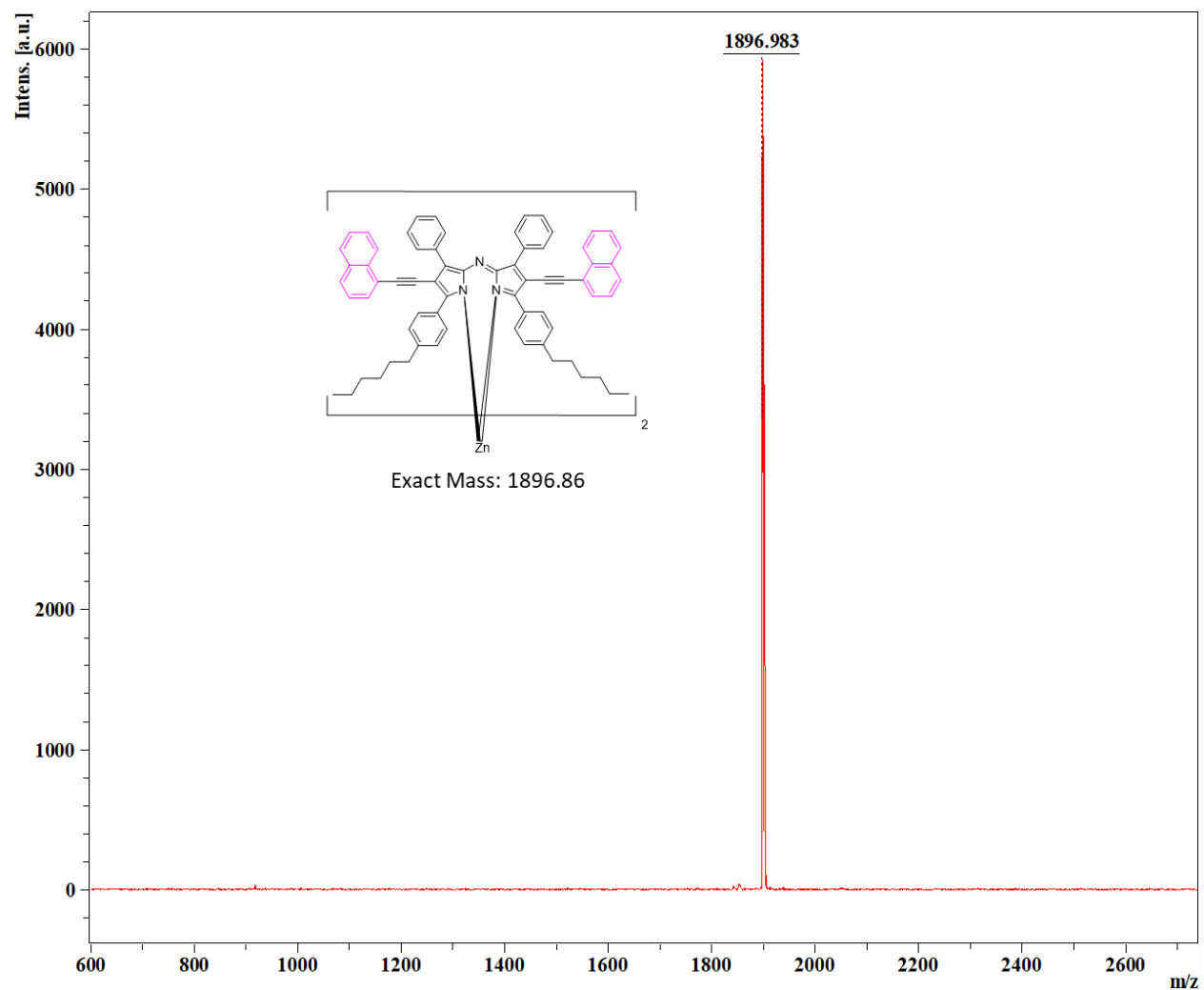
Figure S15. MALDI-TOF mass spectrum of Zn(L2)$_2$.

3. UV-Vis Spectra, TGA, CV, DSC, XRD
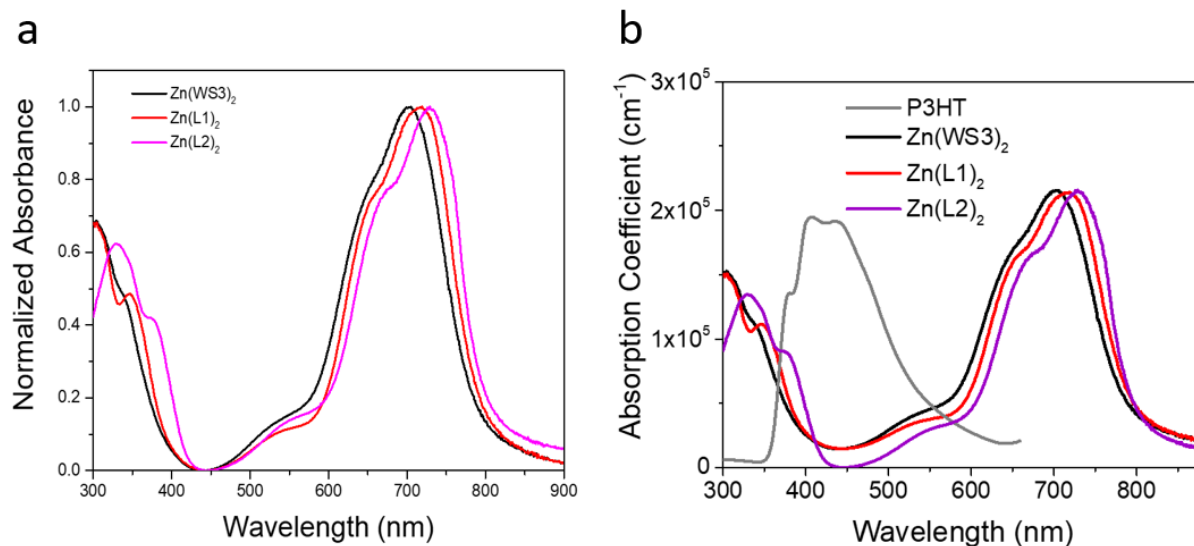
Figure S16. a) Normalized absorbance and b) absorption coefficient of zinc(II) complexes in films. Film thickness were around 50 nm for all materials.
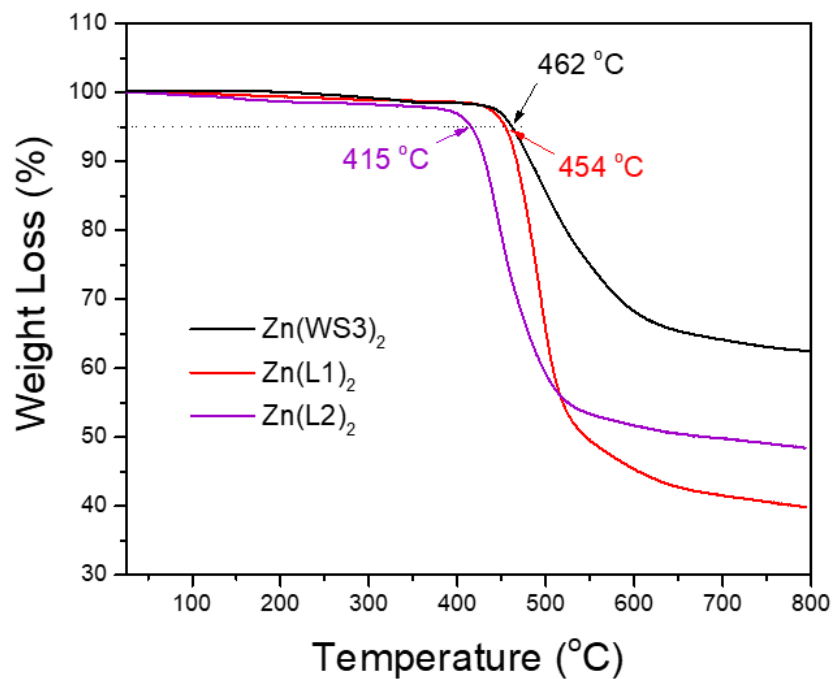
Figure S17. TGA spectra for the zinc(II) complexes.
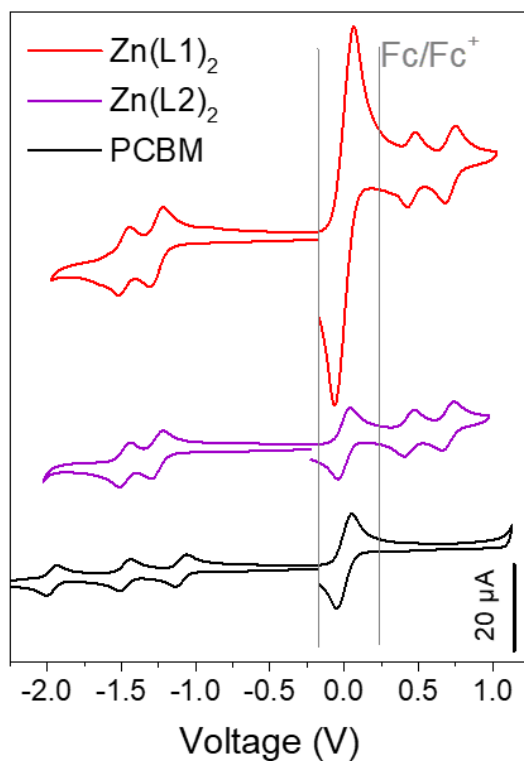
Figure S18. Cyclic voltamograms of Zn complexes and PCBM in 0.1 M TBAPF$_6$ dichloromethane solution with Fc/Fc$^+$ as an internal standard (E$_{1/2}$ at 0.0 V).

Table S1. Electrochemical properties of PCBM and zinc(II) complexes in dichloromethane.

Zinc(II) complexes	E$_{1/2}$ ox. (V)	E(p, a) (V)	E$_{1/2}$ red. (V)	E(p, c) (V)	HOMO/LUMO (eV)	E$_{gap}$ (eV)
Zn (WS3)$_2$*	0.50, 0.77	0.58, 0.86	-1.25, -1.47	-1.33, -1.55	-5.60/-3.85	1.75
Zn(L1)$_2$	0.45, 0.71	0.47, 0.74	-1.26, -1.49	-1.30, -1.52	-5.55/-3.84	1.71
Zn(L2)$_2$	0.44, 0.71	0.47, 0.74	-1.26, -1.48	-1.30, -1.51	-5.54/-3.84	1.70
PCBM	--	--	-1.10, -1.47, -1.97	-1.13, -1.51, -2.00	-5.70/-4.00	1.70*

Note: * Data published before.[5] Estimated HOMO and LUMO energy levels obtained by cyclic voltammetry from the E$_{1/2}$ values in dichloromethane solution, using the value of −5.1 eV for Fc/Fc$^+$ versus vacuum. The HOMO level of PCBM was estimated by using E$_{gap}$ of 1.70 eV. [18]
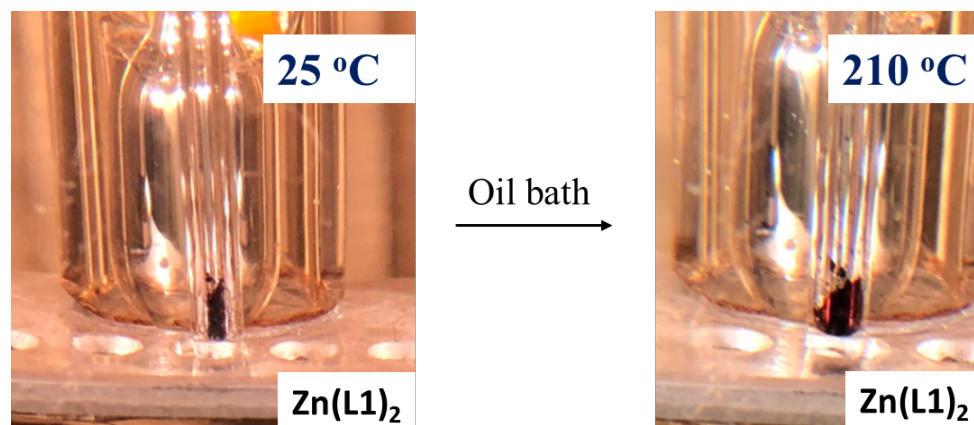
Figure S19. Melting point measurement of Zn(L1)$_2$.
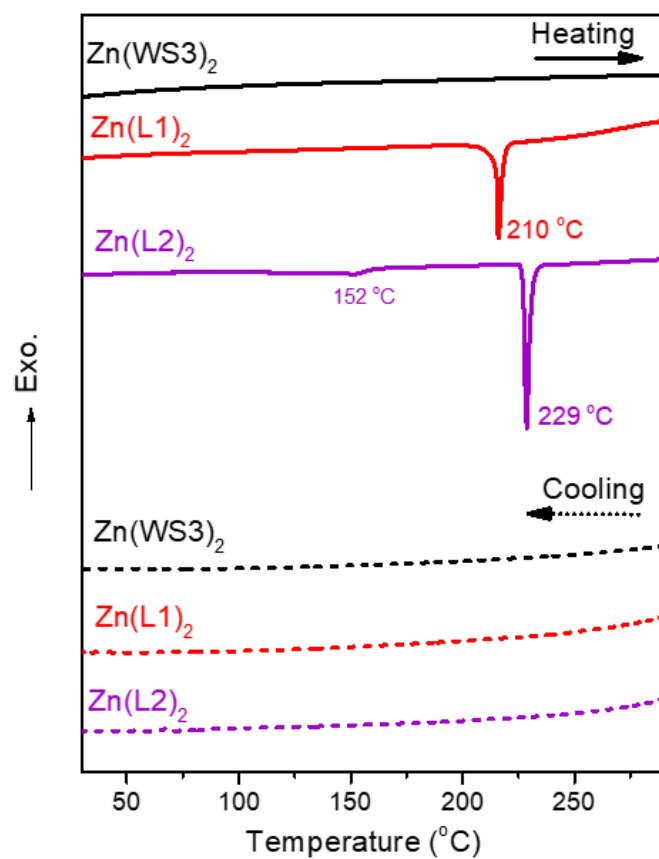
Figure S20. DSC spectra for the zinc(II) complexes with first heating and first cooling cycle.
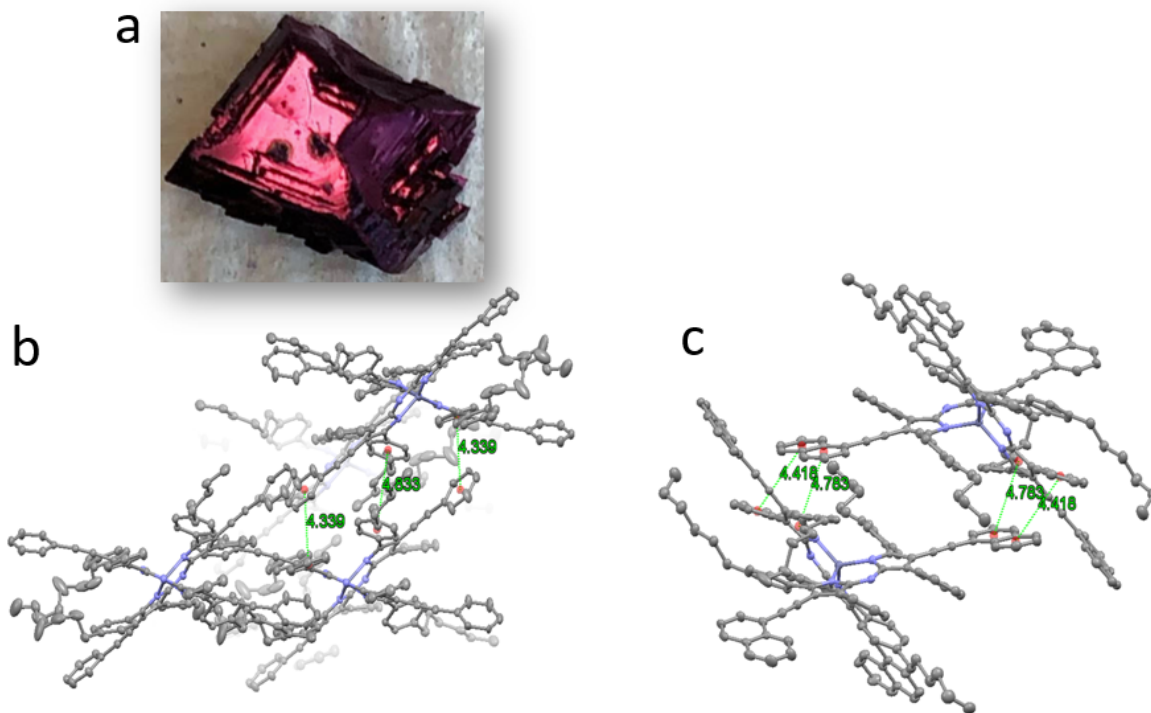
Figure S21. a) Example of Zn(L2)$_2$ crystal grew by evaporating dichloromethane from acetonitrile. b) and c). Intermolecular π-π stacking for b) Zn(L1)$_2$ and for c) Zn(L2)$_2$. Data and figures are extracted from single crystal XRD files by using Mercury 3.10.2.

a HOMO (−5.34 eV)
0% Zn
62% Azadipyrromethene
38% Alkynyl

b HOMO − 1 (−5.36 eV)
0% Zn
62% Azadipyrromethene
38% Alkynyl

c LUMO + 1 (− 3.22 eV)
0% Zn
92% Azadipyrromethene
8% Alkynyl

d LUMO (− 3.27 eV)
0% Zn
93% Azadipyrromethene
7% Alkynyl
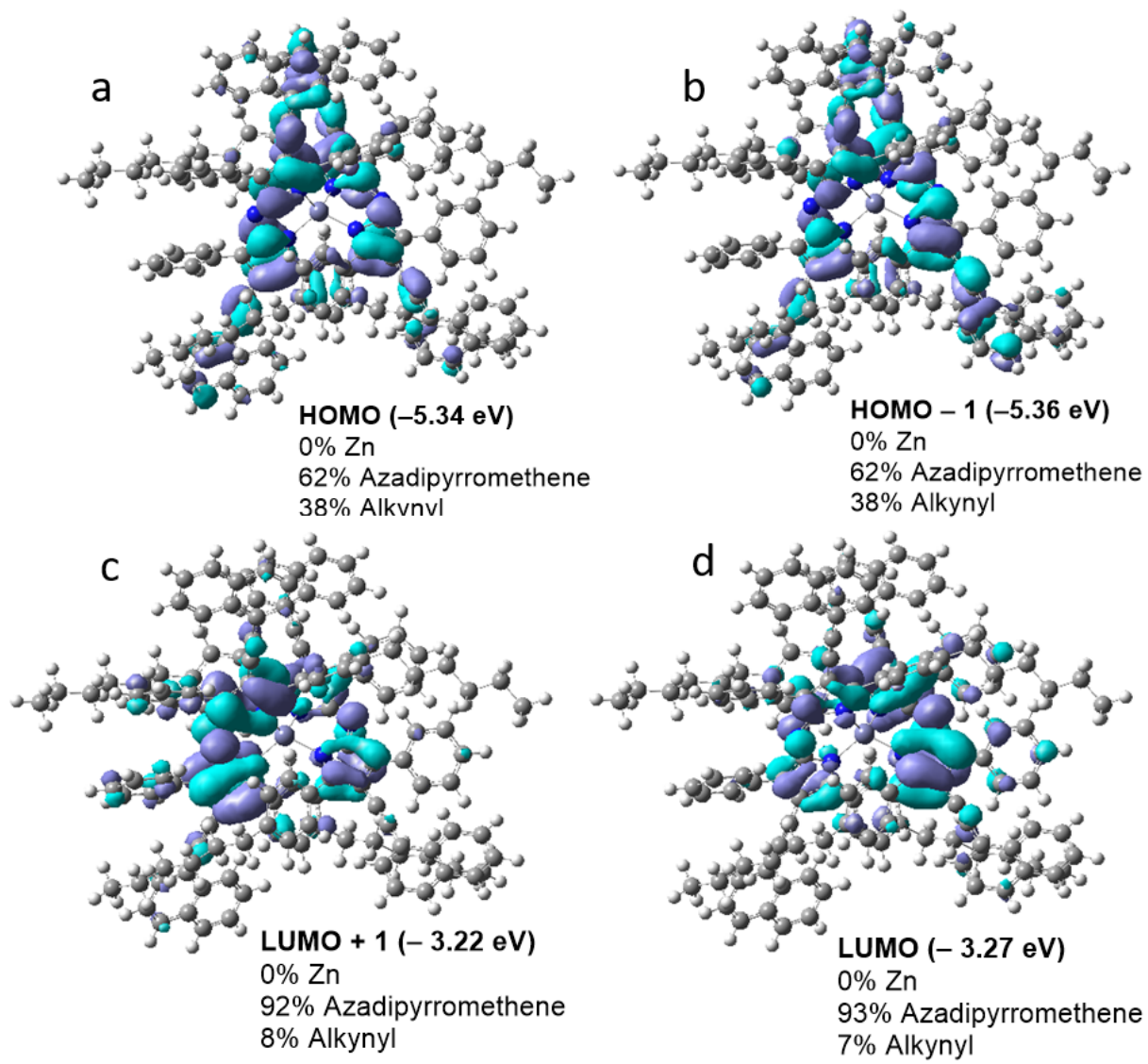
Figure S22. Plots of the a) HOMO − 1, b) HOMO, c) LUMO + 1 and d) LUMO of Zn(L2)$_2$ (contour level 0.02 a.u.). Orbital compositions are expressed as percentages of electron density.

S4

LUMO + 1 ←
   HOMO − 1 55%   S3
LUMO + 1 ←
   HOMO 21%

LUMO ←
   HOMO − 1 44%

LUMO←HOMO 19%   S2
f = 1.09

LUMO + 1 ←
   HOMO 38%
f = 0.92

S1

LUMO + 1 ←
   HOMO 30%
LUMO + 1 ←
   HOMO − 1 30%
LUMO + 1 ←
   HOMO 26%

LUMO←HOMO 58%
LUMO←HOMO − 1 27%
f = 0.016

LUMO←HOMO 12%
f = 0.024

S0
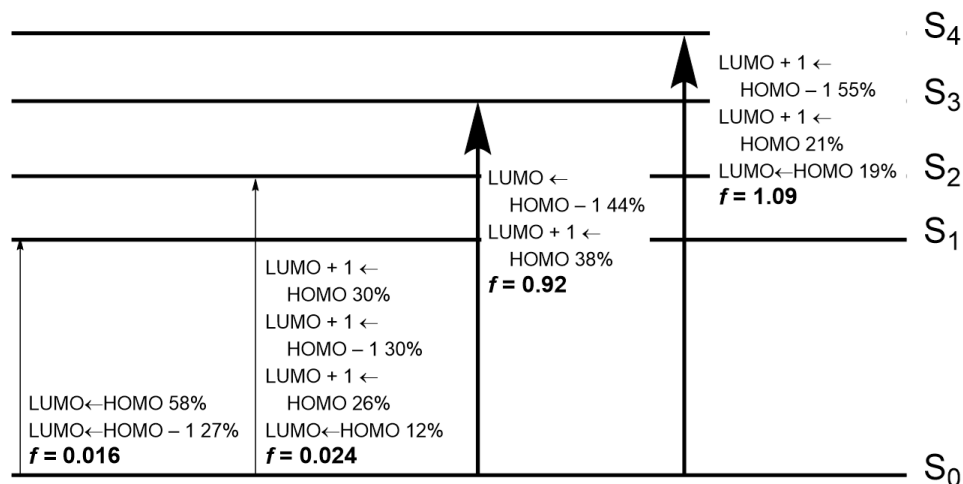
Figure S23. Lowest-lying Franck-Condon singlet excited states of $Zn(L2)_2$ (energies not shown to scale). Percentage composition of vertical transitions and oscillator strengths are indicated to the right of each arrow.
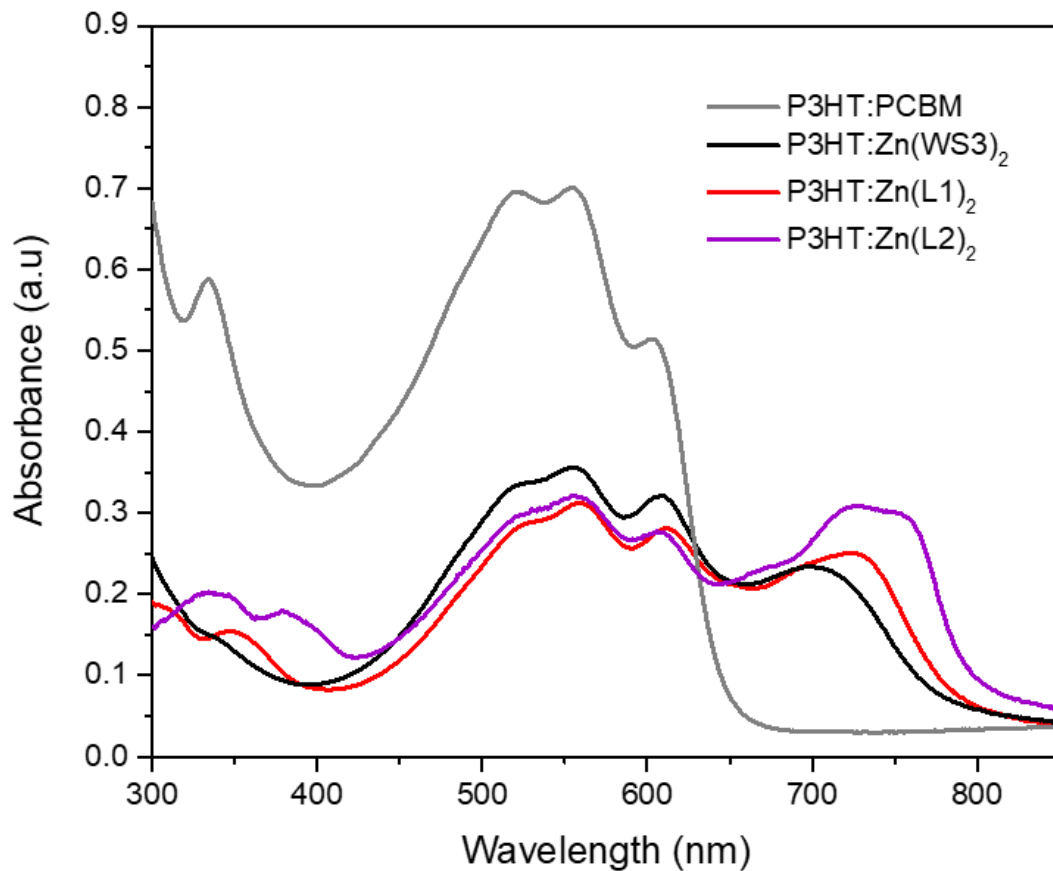
Figure S24. UV-Vis absorption of thin films of zinc(II) complexes by blend with P3HT. Blend ratios are same to the optimized ratio in OPVs in this work. Film thickness of P3HT:zinc(II) complexes blends were around 80 nm and P3HT:PCBM films were around 190 nm.

4. OPV optimization

Table S2. Blend ratio optimization of $Zn(L1)_2$ OPVs.

Ratio of P3HT:$Zn(L1)_2$	J_{sc} (mA/cm^2)	V_{oc} (V)	FF	PCE (%)
1:0.6	4.90	0.75	0.39	1.42
1:0.7	6.10	0.77	0.41	1.92
1:0.8	6.87	0.81	0.44	2.42
1:0.9	6.39	0.81	0.44	2.25
1:1.1	6.37	0.80	0.41	2.09

Note: All cells using the total concentration of 20 mg/mL and annealing condition of 120 °C for 15 mins. Reported PCEs are maximum values obtained.

Table S3. Concentration optimization of $Zn(L1)_2$ OPVs.

Total concentration (mg/mL)	J_{sc} (mA/cm^2)	V_{oc} (V)	FF	PCE (%)
10	6.59	0.80	0.46	2.43
15	7.22	0.79	0.46	2.62
20	6.87	0.81	0.44	2.42
25	7.12	0.82	0.42	2.46
30	5.90	0.81	0.39	1.83

Note: All cells using blend ratio of 1:0.8 between P3HT and $Zn(L1)_2$ and annealing condition of 120 °C for 15 mins. Reported PCEs are maximum values obtained.

Table S4. Annealing condition optimization of $Zn(L1)_2$ OPVs.

Annealing Temperature (°)	Annealing time (min)	J_{sc} (mA/cm^2)	V_{oc} (V)	FF	PCE (%)
As-cast	0	6.41	0.82	0.40	2.12
100	15	6.99	0.79	0.45	2.50
120	15	7.47	0.81	0.49	2.97
140	15	6.89	0.81	0.51	2.84

Note: All cells using blend ratio of 1:0.8 between P3HT and $Zn(L1)_2$ and total concentration of 15 mg/mL. Reported PCEs are maximum values obtained.

Table S5. Blend ratio optimization of Zn(L2)$_2$ OPVs.

Ratio of P3HT:Zn(L2)$_2$	J_{sc} (mA/cm^2)	V_{oc} (V)	FF	PCE (%)
1:0.5	10.29	0.83	0.48	4.11
1:0.6	11.86	0.83	0.50	4.86
1:0.7	11.21	0.83	0.48	4.44
1:0.8	11.18	0.83	0.53	4.87
1:0.9	11.49	0.82	0.53	4.96
1:1	10.06	0.82	0.57	4.70
1:1.1	11.57	0.82	0.56	5.35
1:1.2	9.26	0.83	0.61	4.74
1:1.3	11.33	0.82	0.59	5.51
1:1.4	11.08	0.82	0.56	5.09
1:1.5	9.62	0.80	0.58	4.46

Note: All cells using the total concentration of 20 mg/mL and annealing condition of 120 ºC for 15 mins. Reported PCEs are maximum values obtained.

Table S6. Concentration optimization of Zn(L2)$_2$ OPVs

Total concentration (mg/mL)	J_{sc} (mA/cm^2)	V_{oc} (V)	FF	PCE (%)
15	9.29	0.81	0.62	4.64
20	11.33	0.82	0.59	5.51
25	11.34	0.82	0.54	5.02

Note: All cells using blend ratio of 1:1.3 between P3HT and Zn(L2)$_2$ and annealing condition of 120 ºC for 15 mins. Reported PCEs are maximum values obtained.

Table S7. Annealing condition optimization of $Zn(L2)_2$ OPVs.

Annealing Temperature (^{o})	Annealing time (min)	J_{sc} (mA/cm^2)	V_{oc} (V)	FF	PCE (%)
As-cast	0	9.40	0.81	0.48	3.64
100	15	9.49	0.82	0.52	4.01
120	15	10.82	0.81	0.59	5.17
140	15	9.11	0.83	0.62	4.66
160	15	8.01	0.81	0.59	3.83

Note: All cells using blend ratio of 1:1 between P3HT and $Zn(L2)_2$ and total concentration of 20 mg/mL. Reported PCEs are maximum values obtained.

Table S8. Optimized fabrication conditions and performances for OPVs.

P3HT: Acceptor	Ratio	Total Concentration (mg mL^{-1})	Annealing Temperature (^{o}C)	Annealing Time (min)	Active Layer Thickness (nm)	Maximum PCE
$Zn(WS3)_2$	1:0.7	20	120	30	85	2.5%
$Zn(L1)_2$	1:0.8	15	100	15	70	3.0%
$Zn(L2)_2$	1:1.3	20	120	15	80	5.5%
PCBM	1:0.8	40	120	30	190	4.1%

5. Mobility measurement by SCLC and TFT
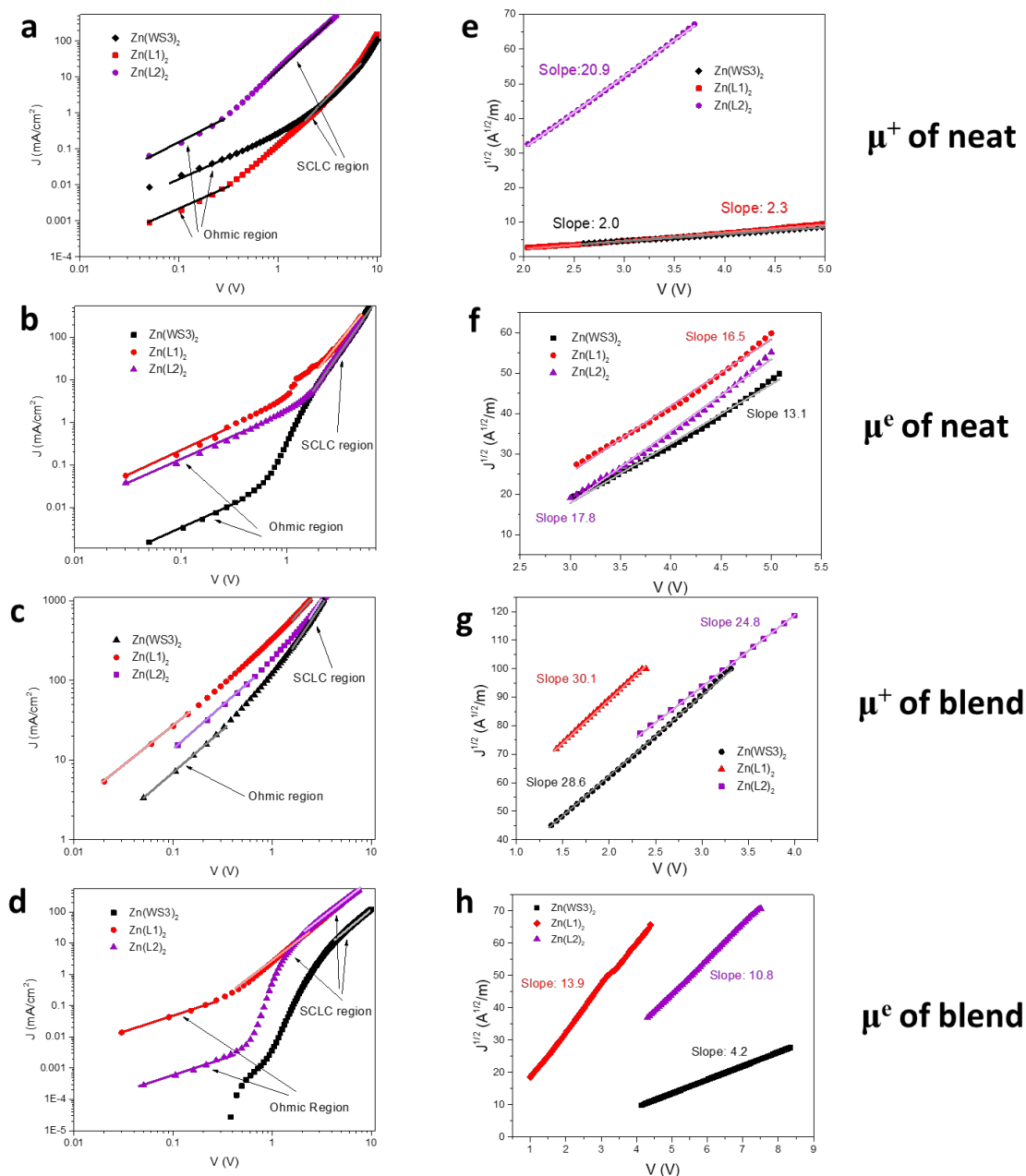
Figure S25. SCLC mobility of zinc(II) complexes by plotting the double logarithm relationship between J and absolute V of: a) hole-only mobility in neat films; b) electron-only mobility in neat films; c) hole-only mobility in P3HT:zinc(II) complexes blend films; d) electron-only mobility in P3HT:zinc(II) complexes blend films. The data in the range of SCLC region shows fits to the Mott-Gurney law. e) $J^{1/2}$ characteristics of hole-only mobility in neat films. f) $J^{1/2}$ characteristics of electron-only mobility in neat films. g) $J^{1/2}$ characteristics of hole-only mobility in P3HT:zinc(II) complexes blend films. h) $J^{1/2}$ characteristics of electron-only mobility in P3HT:acceptor blend films.
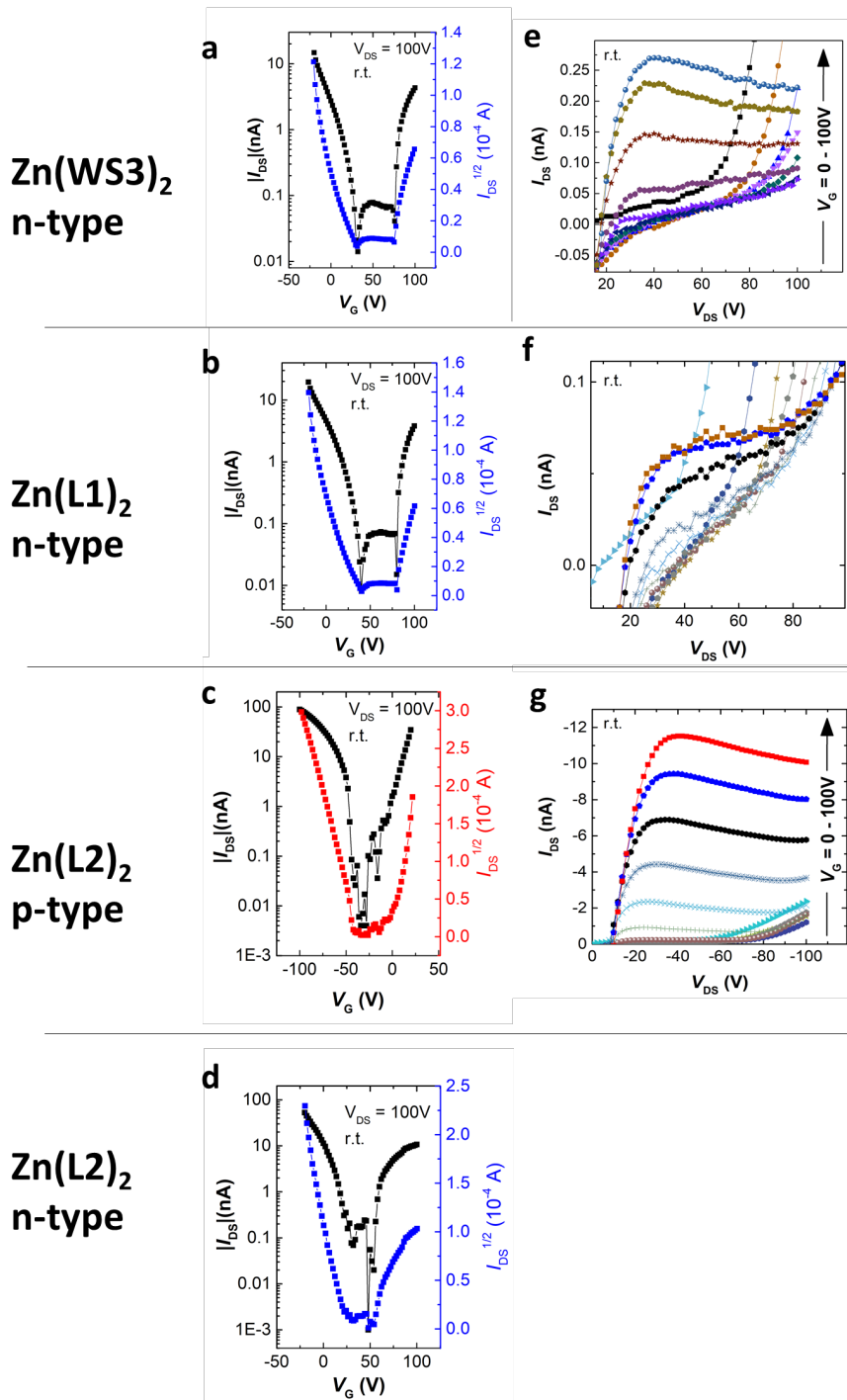
Figure S26. Thin film Transistor (TFT) measurements of zinc(II) complexes in neat films. a), b), c) and d) are the transfer characteristics of zinc(II) complexes by plotting the semi-logarithmic relationship betweeen drain-to-source current (I_{DS}) and gate voltage (V_G) and the linaer relationship between root square of I_{DS} and V_G. e), f) and g) are the output characteritics of zinc(II) complexes by plotting the linear relationship between I_{DS} and drain-to-source voltage (V_{DS}) by varing the V_G. V_G step voltage is 10 V for all output characteristics. We are not able to obtain output characteristics of Zn(L2)$_2$.

Table S9. Summarized parameters for zinc(II) complexes in TFT.

Neat film	Transistor Type	Max. μ_{sat} $(cm^2V^{-1}s^{-1})$	Avg. ($\pm$ Std) $\mu_{sat}(cm^2V^{-1}s^{-1})$	Avg. ($\pm$ Std) V_T	Avg. $I_{on/off}$
Zn(WS3)$_2$	n-type	2.92×10^{-5}	$(2.26 \pm 0.07) \times 10^{-5}$	(71 ± 5)	5.5×10^2
Zn(L1)$_2$	n-type	4.7×10^{-5}	$(4.6 \pm 0.6) \times 10^{-5}$	(79 ± 7)	7.0×10^2
Zn(L2)$_2$	n-type	1.5×10^{-4}	$(6.8 \pm 7.5) \times 10^{-5}$	(46 ± 7)	7.0×10^2
	p-type	1.3×10^{-4}	$(1.3 \pm 0.3) \times 10^{-4}$	(37 ± 5)	1.0×10^4

Note: μ_{sat} is saturation mobility, V_T is threshold voltage and $I_{on/off}$ is on-to-off current ratio.

6. Film characterizations
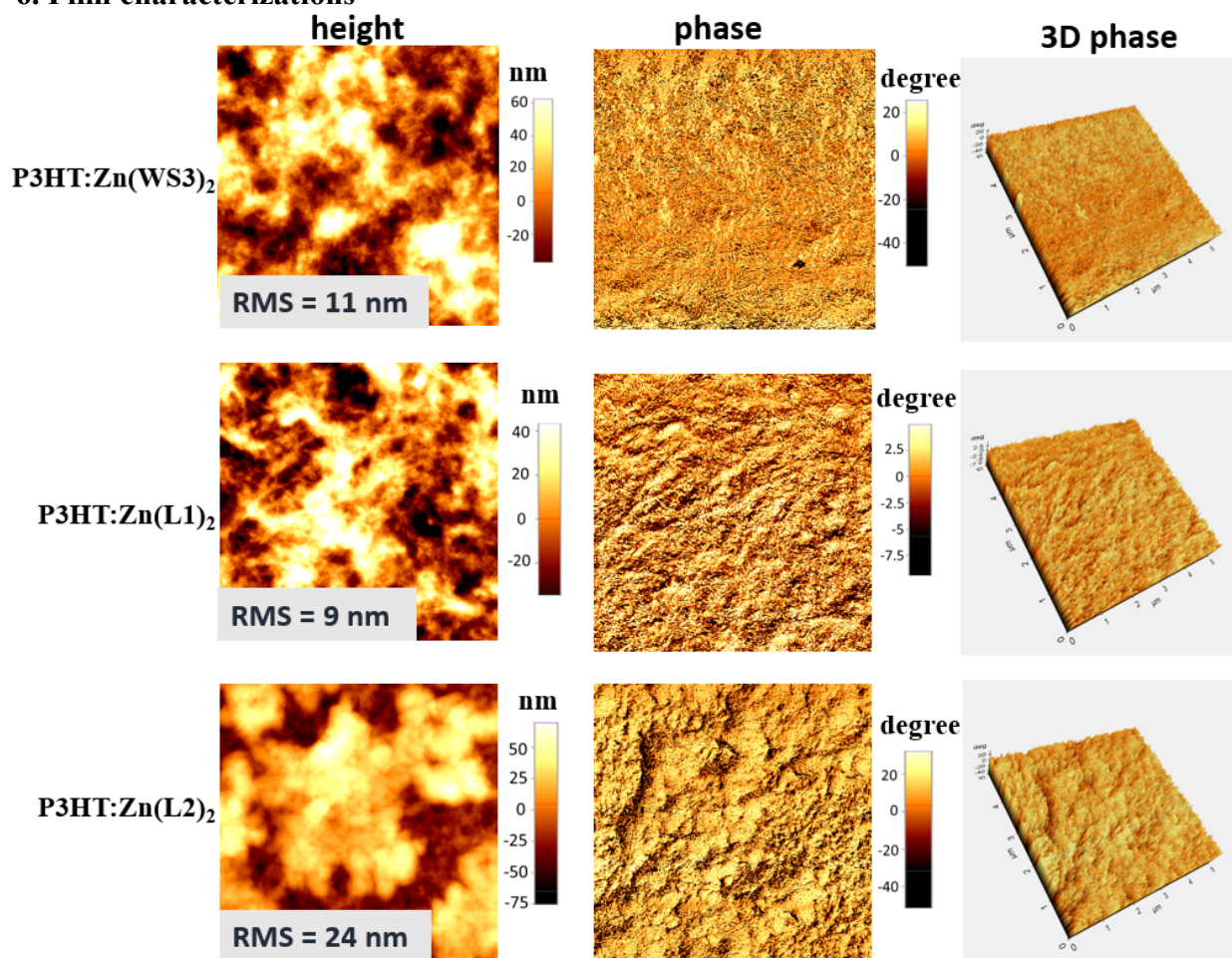
Figure S27. 5 × 5 μm AFM phase, height and 3D phase images for P3HT:Zn(WS3)$_2$, P3HT:Zn(L1)$_2$ and P3HT:Zn(L2)$_2$ blend films respectively. In phase images, dark and bright parts can be differentiated as different components. Roughness for 5 × 5 μm images were shown on the phase images. The roughness calculated from 5 × 5 μm images follow the same trend as the roughness calculated from 1 × 1 μm images.
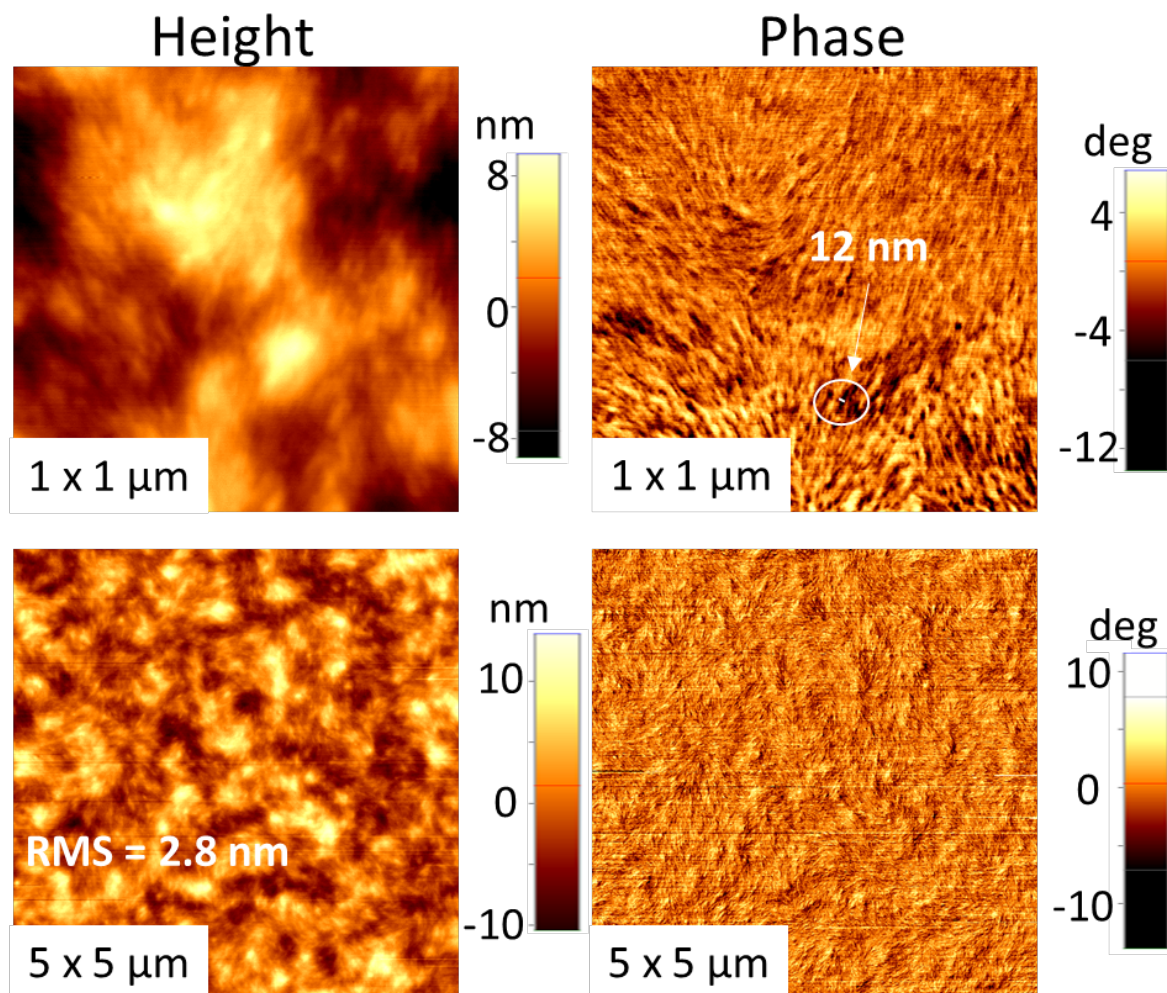
Figure S28. 1×1 μm and 5×5 μm AFM phase and height images for Zn(L2)$_2$:P(NDI2OD-T2) blend films. In phase images, dark and bright parts can be differentiated as different components. Roughness for 5×5 μm images were shown on the phase images. The domain size is around 12 nm, larger than the reported diffusion length of P(NDI2OD-T2) of 1.1 nm.[19]
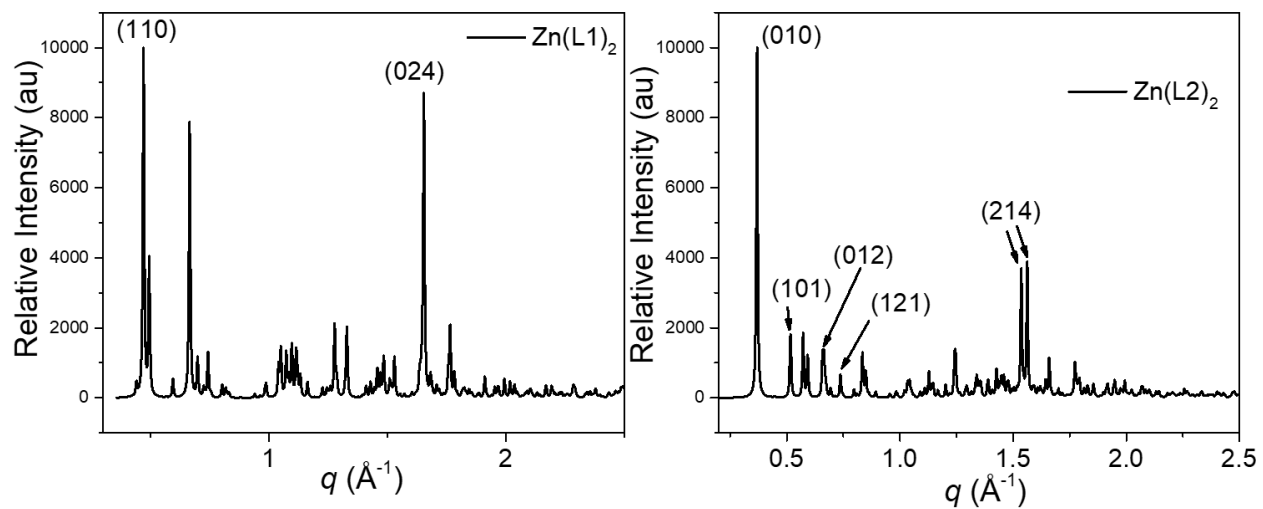
Figure S29. Powder diffraction patterns of Zn(L1)$_2$ and Zn(L2)$_2$ calculated from the correspond single crystal structures.
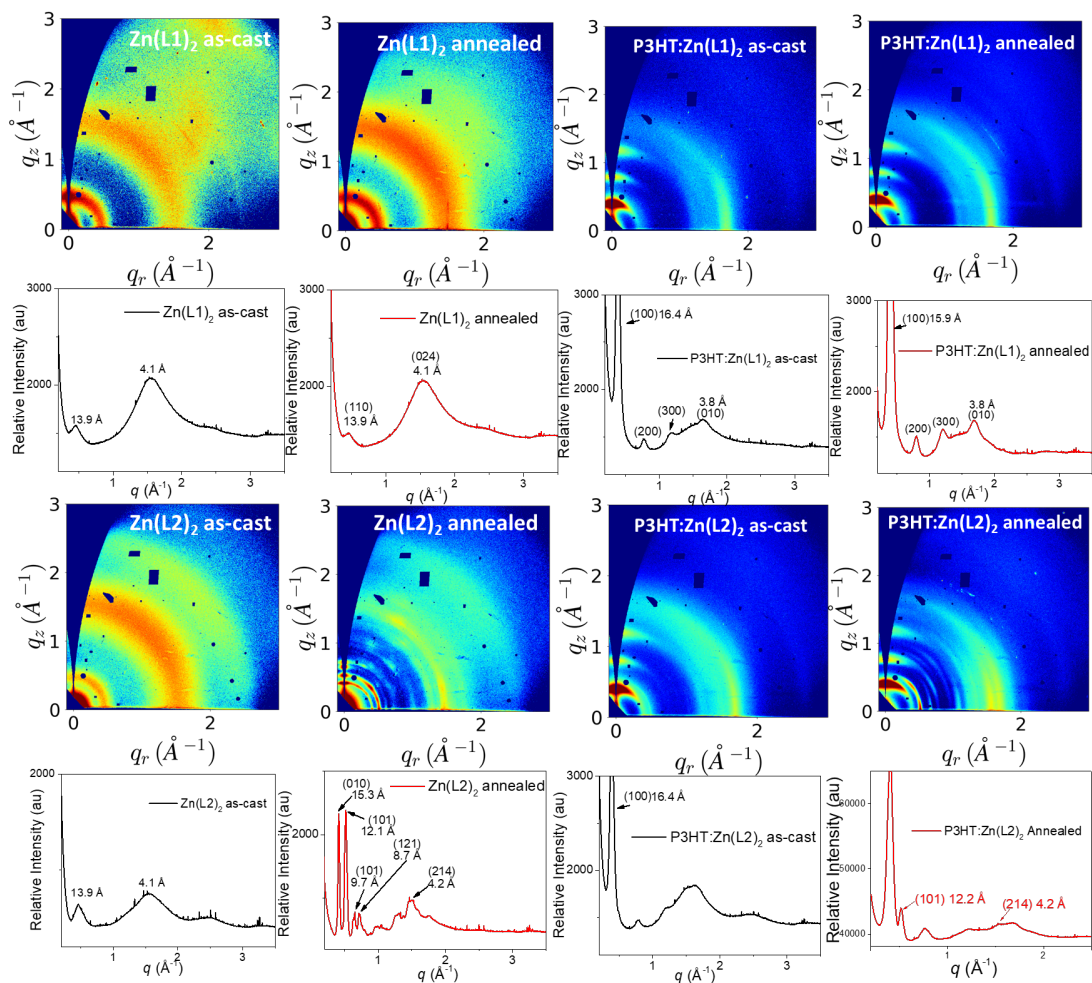
Figure S30. 2D GI-WAXD images of $Zn(L1)_2$ and $Zn(L2)_2$ neat films, P3HT:$Zn(L1)_2$ and P3HT:$Zn(L2)_2$ blend films with or without thermal annealing. Graphs are the corresponding intensity profiles along q_r axis for GI-WAXD images.
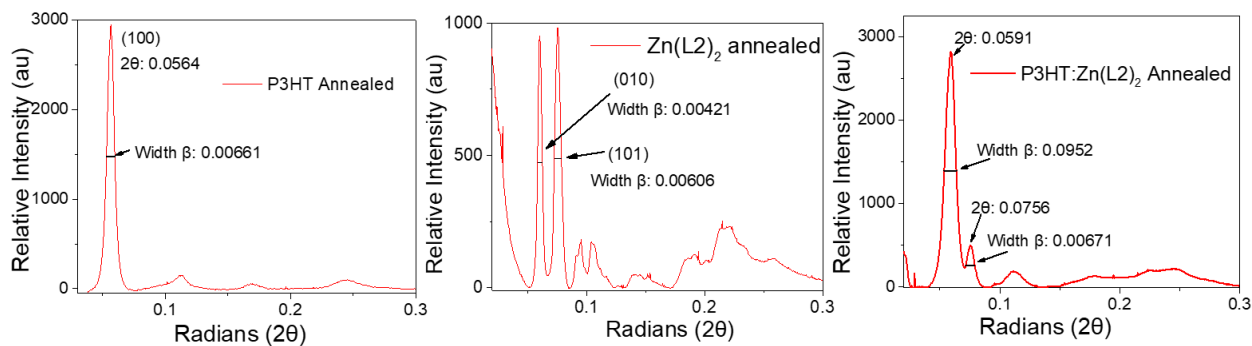
Figure S31. Diffractogram of 2D GI-WAXD images of P3HT and $Zn(L2)_2$ in neat films, and P3HT:$Zn(L2)_2$ in blend film with thermal annealing. The τ_{010} peak of $Zn(L2)_2$ is overlapped with the τ_{100} peak of P3HT in the P3HT:$Zn(L2)_2$ diffractogram. Considering the intensity of τ_{010} peak is much smaller than the τ_{100} peak, we assume the peak overlap at 2θ of 0.0591 in P3HT:$Zn(L2)_2$ have negligible influence on the peak width β.

7. Donor Properties of Zn(L2)₂
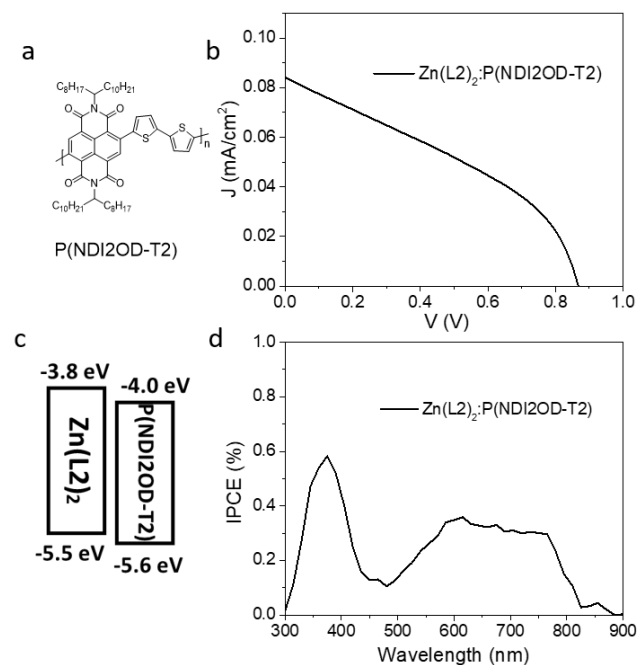
Figure S32. a) Chemical structure of P(NDI2OD-T2); b) Current density–voltage characteristics of Zn(L2)₂:P(NDI2OD-T2) OPVs; c) Energy levels of Zn(L2)₂ and P(NDI2OD-T2); d) Incident photon-to-current efficiency spectra of OPVs.

8. Synthetic complexity and industrial figure of merit analysis
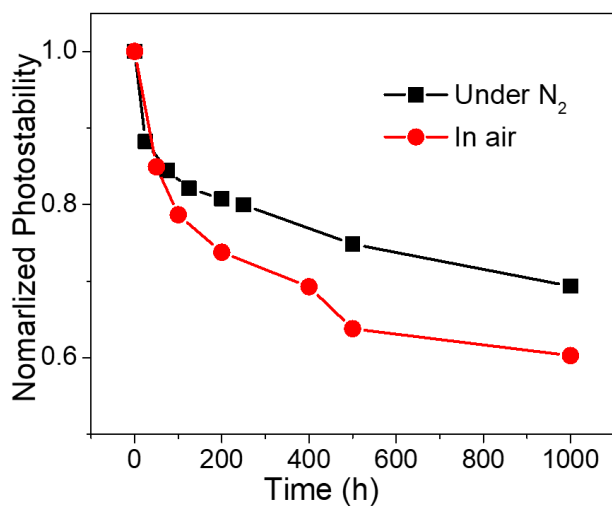
Figure S33. Normalized photostability of P3HT:Zn(L2)₂ cell under N₂ atmosphere and in air.

Table S10. Synthetic parameters of Zn(L1)$_2$ and Zn(L2)$_2$

Material	Synthetic steps (NSS)	Yield	Number of purification steps (NUO)	Columns (NCC)	Number of hazardous chemicals (HNC)
Zn(L1)$_2$	6	30 %	5	1	16
Zn(L2)$_2$	7	43 %	6	0	17
MO-IDIC-2F	6	58 %	11	4	16
PTQ10	4	85 %	6	1	18
PDCBT	5	27%	5	3	17

Table S11. Normalized values of number of synthetic steps (NSS), reciprocal yield (RY), number of operation units for the isolation/purification (NUO), number of chromatograph columns (NCC) and number of hazardous chemicals (NHC) for materials investigated in this work. All values are normalized to the maximal values of polymers.[20] i-FoM shown in the table are for the blended active layers of P3HT and acceptors except for MO-IDIC-2F, PTQ10 and PDCBT. (NSS$_{max}$: 22, RY$_{max}$: 86.9, NUO$_{max}$: 39, NCC$_{max}$: 13, NHC$_{max}$: 44). SC = 35 × NSS/NSS$_{max}$ + 25 × logRY/logRY$_{max}$ + 15 × NUO/NUO$_{max}$ + 15 × NCC/NCC$_{max}$ + 10 × NHC/NHC$_{max}$. i-FoM = PCE × Photostability/SC.

Material	NSS/ NSS$_{max}$	logRY/ logRY$_{max}$	NUO/ NUO$_{max}$	NCC/ NCC$_{max}$	NHC/ NHC$_{max}$	SC index (%)	200 h Stability	i-FoM	Ref.
PC$_{61}$BM	0.23	0.226	0.154	0.154	0.136	20.6	0.92	0.18	[20]
O-IDTBR	0.5	0.267	0.615	0.461	0.364	43.9	0.98	0.23	[21]
Zn(L1)$_2$	0.27	0.268	0.128	0.0769	0.364	22.9	--	--	
Zn(L2)$_2$	0.32	0.188	0.154	0	0.409	22.1	0.81	0.30	
MO-IDIC-2F	0.27	0.123	0.282	0.308	0.364	25.2	--	--	[22]
PTQ10	0.18	0.035	0.154	0.0769	0.41	14.8	--	--	[23]
PDCBT	0.23	0.29	0.128	0.231	0.409	24.8	--	--	[24]

9. Crystal data for Zn(L1)$_2$ and Zn(L2)$_2$

Table S12. Crystal data and structure refinement for Zn(L1)$_2$.

Identification code	Zn(L1)$_2$
Empirical formula	C120 H108 N6 Zn
Formula weight	1699.49
Temperature	100.0 K
Wavelength	0.71073 Å
Crystal system	Monoclinic
Space group	C 2/c
Unit cell dimensions	a = 31.907(18) Å = 90°.

	b = 17.264(10) Å	= 138.456(6)°.
	c = 25.540(14) Å	= 90°.
Volume	9330(9) Å^3	
Z	4	
Density (calculated)	1.210 Mg/m^3	
Absorption coefficient	0.318 mm^{-1}	
F(000)	3600	
Crystal size	0.3 x 0.26 x 0.23 mm^3	
Theta range for data collection	1.425 to 24.997°.	
Index ranges	-37<=h<=37, -15<=k<=20, -29<=l<=30	
Reflections collected	28248	
Independent reflections	8191 [R(int) = 0.0248]	
Completeness to theta = 24.997°	99.7 %	
Absorption correction	Semi-empirical from equivalents	
Max. and min. transmission	0.7454 and 0.6274	
Refinement method	Full-matrix least-squares on F^2	
Data / restraints / parameters	8191 / 0 / 615	
Goodness-of-fit on F^2	1.126	
Final R indices [I>2sigma(I)]	R1 = 0.0492, wR2 = 0.1187	
R indices (all data)	R1 = 0.0647, wR2 = 0.1330	
Extinction coefficient	n/a	
Largest diff. peak and hole	0.818 and -0.418 e.Å^{-3}	

Table S13. Crystal data and structure refinement for Zn(L2)$_2$.

Identification code	Zn(L2)$_2$	
Empirical formula	C137 H118 Cl2 N6 Zn	
Formula weight	1984.64	
Temperature	100.0 K	
Wavelength	0.71073 Å	
Crystal system	Triclinic	
Space group	P-1	
Unit cell dimensions	a = 15.784(9) Å	= 73.986(7)°.
	b = 19.232(11) Å	= 89.616(6)°.
	c = 19.802(11) Å	= 68.125(7)°.
Volume	5331(5) Å^3	
Z	2	
Density (calculated)	1.236 Mg/m^3	
Absorption coefficient	0.337 mm^{-1}	
F(000)	2092	
Crystal size	0.33 x 0.29 x 0.27 mm^3	
Theta range for data collection	1.076 to 25.923°.	
Index ranges	-19<=h<=19, -23<=k<=23, -24<=l<=24	

Reflections collected   87310
Independent reflections   20198 [R(int) = 0.0557]
Completeness to theta = 25.242°   99.7 %
Absorption correction   Semi-empirical from equivalents
Max. and min. transmission   0.7452 and 0.5668

Refinement method   Full-matrix least-squares on F^2
Data / restraints / parameters   20198 / 0 / 1319

Goodness-of-fit on F^2 1.065
Final R indices [I>2sigma(I)]   R1 = 0.0855, wR2 = 0.2278
R indices (all data)   R1 = 0.1082, wR2 = 0.2458
Extinction coefficient   n/a
Largest diff. peak and hole   1.955 and -0.997 e.Å^{-3}

Table S14. Cartesian Coordinates (Å) of Zn(L1)$_2$

235

C	-3.607717	-1.695887	-0.243331
C	-2.845404	-2.578654	-1.026980
C	-1.510272	-2.017105	-1.124874
N	-1.442199	-0.853016	-0.450371
C	-2.711238	-0.633016	0.145856
N	-3.013541	0.344392	0.979168
C	-2.250730	1.282983	1.504316
N	-0.863207	1.475531	1.240409
C	-0.428563	2.423167	2.096062
C	-1.514700	2.899015	2.928829
C	-2.666163	2.193900	2.547514
C	-5.027774	-1.807329	0.108757
C	-4.014377	2.310631	3.104717
C	-5.519110	-1.320596	1.338876
C	-6.869311	-1.444184	1.662712
C	-7.761192	-2.046805	0.770509
C	-7.289420	-2.522459	-0.457526
C	-5.939674	-2.406725	-0.785411
C	-5.155116	2.092604	2.305240
C	-6.433506	2.218630	2.846920
C	-6.603599	2.559130	4.191060
C	-5.480528	2.771643	4.995642
C	-4.200327	2.651682	4.460516
C	-1.397691	3.938131	3.867086
C	-1.253072	4.855621	4.651227
C	-1.057689	5.926442	5.564461
C	-3.265925	-3.792602	-1.596062
C	-3.626944	-4.849767	-2.076393

```
C    -4.057769   -6.086099   -2.629442
C    -2.139866    6.461455    6.294364
C    -1.933143    7.508593    7.188780
C    -0.652633    8.039470    7.371436
C     0.425681    7.516737    6.650651
C     0.231219    6.469955    5.753554
C    -3.280327   -6.745813   -3.604879
C    -3.708702   -7.957472   -4.141141
C    -4.912254   -8.531132   -3.719632
C    -5.688976   -7.884618   -2.753320
C    -5.270621   -6.673058   -2.209059
C    -0.383638   -2.599087   -1.855839
C     0.954359    2.899626    2.179666
C    -0.155533   -3.987797   -1.832164
C     0.929389   -4.536563   -2.510028
C     1.814918   -3.727808   -3.237395
C     1.582638   -2.345524   -3.263771
C     0.503476   -1.786916   -2.585405
C     1.588714    2.997251    3.432846
C     2.909754    3.425216    3.521796
C     3.635378    3.778811    2.373369
C     2.993956    3.698872    1.130123
C     1.672493    3.267811    1.031780
C     3.026397   -4.325746   -3.925696
C     4.246493   -4.388495   -2.965735
C     5.498339   -4.987173   -3.643079
C     6.711444   -5.035816   -2.688705
C     7.979037   -5.615590   -3.353504
C     9.180321   -5.643901   -2.383892
C     5.095459    4.176583    2.475025
C     6.015262    2.925209    2.523705
C     7.513452    3.292878    2.586272
C     8.419264    2.041666    2.608461
C     9.923268    2.391140    2.643269
C    10.811586    1.128196    2.646331
C     1.972025    1.654045   -1.852985
C     2.182394    2.735259   -2.782437
C     0.905711    3.250894   -3.079163
C    -0.051974    2.456309   -2.345026
N     0.578214    1.518847   -1.602431
N     2.931519    0.931334   -1.294165
C     2.848557   -0.017253   -0.386138
N     1.652269   -0.450511    0.248296
C     1.963547   -1.513556    1.006462
C     3.387034   -1.797258    0.929194
C     3.951329   -0.843932    0.068359
```

```
C    3.475215   3.204627  -3.288628
C    5.357028  -0.694618  -0.315152
C    4.545804   2.311216  -3.498976
C    5.765341   2.770313  -3.993295
C    5.947096   4.124990  -4.284019
C    4.896395   5.021867  -4.073041
C    3.673079   4.569272  -3.583165
C    6.234598  -1.799091  -0.285228
C    7.578448  -1.653399  -0.624628
C    8.080774  -0.405371  -1.003751
C    7.221243   0.695947  -1.047907
C    5.875689   0.557764  -0.709379
C    4.029324  -2.790240   1.686674
C    4.534691  -3.647459   2.385589
C    5.099448  -4.657546   3.209845
C    0.567388   4.263222  -3.993145
C    0.229409   5.115019  -4.791675
C   -0.185404   6.107804  -5.719835
C    4.265127  -5.461839   4.016027
C    4.815162  -6.454733   4.822153
C    6.197674  -6.664162   4.841617
C    7.031878  -5.870740   4.048209
C    6.493156  -4.874687   3.237802
C    0.760818   6.823169  -6.483414
C    0.341653   7.795980  -7.387331
C   -1.019579   8.072278  -7.547283
C   -1.964782   7.366273  -6.796584
C   -1.557535   6.391449  -5.889790
C   -1.508925   2.573900  -2.428498
C    0.974407  -2.269400   1.773461
C   -2.147962   3.824208  -2.364279
C   -3.535161   3.912295  -2.474140
C   -4.320768   2.767530  -2.670758
C   -3.677584   1.522726  -2.738995
C   -2.296189   1.423361  -2.615896
C   -0.044367  -1.614788   2.486459
C   -1.044085  -2.345352   3.122142
C   -1.061072  -3.746452   3.064504
C   -0.024331  -4.397908   2.379756
C    0.983681  -3.676057   1.746430
C   -5.831259   2.851111  -2.799233
C   -6.562152   2.274655  -1.556299
C   -8.097094   2.282648  -1.728124
C   -8.830387   1.665740  -0.517403
C  -10.363988   1.634292  -0.696592
C  -11.078162   1.005446   0.519326
```

```
C    -2.225353   -4.531917    3.635474
C    -3.342036   -4.687627    2.564910
C    -4.565540   -5.478575    3.073970
C    -5.656258   -5.600264    1.986535
C    -6.906266   -6.370353    2.464464
C    -7.977775   -6.467032    1.356733
Zn   -0.025246    0.408337   -0.139206
H    -4.840277   -0.829197    2.019003
H    -7.223648   -1.060651    2.612378
H    -8.810966   -2.139515    1.025535
H    -7.974957   -2.977572   -1.163421
H    -5.585660   -2.769140   -1.740844
H    -5.028720    1.822287    1.266991
H    -7.296879    2.054052    2.213061
H    -7.599508    2.658249    4.607575
H    -5.602783    3.025798    6.042443
H    -3.335075    2.808937    5.090250
H    -3.130144    6.049279    6.144725
H    -2.771462    7.913645    7.743738
H    -0.496676    8.854925    8.067897
H     1.419041    7.928086    6.787979
H     1.059833    6.060679    5.188635
H    -2.350608   -6.294297   -3.928654
H    -3.104767   -8.455662   -4.890727
H    -5.241687   -9.473870   -4.140351
H    -6.621583   -8.327122   -2.422533
H    -5.865156   -6.170150   -1.456043
H    -0.817544   -4.625687   -1.262860
H     1.096766   -5.608147   -2.472748
H     2.249358   -1.701396   -3.827407
H     0.336476   -0.718452   -2.637789
H     1.045892    2.721060    4.327728
H     3.391260    3.478270    4.492810
H     3.528770    3.982064    0.229718
H     1.181537    3.247221    0.069512
H     2.794757   -5.339264   -4.276799
H     3.292544   -3.721890   -4.802072
H     4.469804   -3.376398   -2.605827
H     3.977547   -4.992064   -2.089143
H     5.272079   -6.002631   -3.997939
H     5.756997   -4.383948   -4.524669
H     6.924668   -4.019163   -2.332737
H     6.455423   -5.643015   -1.808870
H     7.768672   -6.633162   -3.708806
H     8.231583   -5.010187   -4.234180
H    10.075460   -6.045817   -2.871451
```

H	9.409265	-4.631467	-2.029202
H	8.955091	-6.267923	-1.510986
H	5.373358	4.791824	1.610460
H	5.258971	4.777540	3.378823
H	5.746967	2.319621	3.398932
H	5.827987	2.308938	1.636479
H	7.771144	3.909027	1.712976
H	7.706240	3.901120	3.481495
H	8.170255	1.430228	3.486962
H	8.210195	1.432204	1.719454
H	10.168393	3.010298	1.769675
H	10.135567	2.993847	3.536542
H	11.875464	1.390679	2.660326
H	10.598288	0.511340	3.527243
H	10.616749	0.522682	1.753260
H	4.414090	1.265958	-3.261787
H	6.573672	2.065943	-4.152924
H	6.896475	4.478284	-4.669830
H	5.031851	6.076297	-4.285556
H	2.865862	5.269718	-3.415469
H	5.854505	-2.771048	-0.003057
H	8.233168	-2.517413	-0.599022
H	9.126538	-0.294190	-1.266506
H	7.594831	1.667454	-1.350600
H	5.211995	1.407359	-0.764136
H	3.195833	-5.290071	3.997713
H	4.166182	-7.065905	5.438654
H	6.621455	-7.437357	5.471601
H	8.104124	-6.028306	4.063751
H	7.135113	-4.253402	2.625584
H	1.813400	6.600871	-6.358668
H	1.076569	8.339193	-7.970101
H	-1.341211	8.829658	-8.252445
H	-3.020935	7.575963	-6.920643
H	-2.282963	5.836680	-5.307406
H	-1.557039	4.718998	-2.215916
H	-4.016204	4.882380	-2.407495
H	-4.263910	0.624470	-2.899445
H	-1.816002	0.458158	-2.696547
H	-0.040460	-0.534109	2.548428
H	-1.826330	-1.822963	3.662840
H	-0.022254	-5.481749	2.326063
H	1.757951	-4.192068	1.194333
H	-6.133907	3.895318	-2.943419
H	-6.152132	2.289051	-3.686759
H	-6.222621	1.245281	-1.383655

```
H   -6.282374    2.862512   -0.672931
H   -8.444383    3.314385   -1.879250
H   -8.359291    1.715429   -2.632604
H   -8.463260    0.643811   -0.354022
H   -8.586357    2.244538    0.384663
H  -10.732476    2.656968   -0.852449
H  -10.606658    1.061214   -1.601471
H  -12.163560    0.977814    0.372073
H  -10.726379   -0.020656    0.680053
H  -10.870094    1.582409    1.428262
H   -1.889980   -5.525956    3.956788
H   -2.635619   -4.015536    4.512122
H   -3.663395   -3.691089    2.240048
H   -2.921207   -5.189065    1.684107
H   -4.250510   -6.482496    3.392351
H   -4.986680   -4.972992    3.954484
H   -5.954757   -4.594657    1.663783
H   -5.232139   -6.109178    1.109394
H   -6.613589   -7.379069    2.785430
H   -7.329697   -5.860679    3.340302
H   -8.869253   -6.999048    1.707732
H   -8.276871   -5.463961    1.030856
H   -7.579698   -7.003365    0.486338
```

Table S15. Cartesian Coordinates of Zn(L2)$_2$

259

```
C   -2.845164   -0.750530    0.163675
C   -3.773663   -1.770778   -0.254562
C   -3.052832   -2.614241   -1.112575
C   -1.712979   -2.076528   -1.194903
N   -1.606142   -0.962784   -0.454698
N   -3.158051    0.194778    1.032915
C   -2.403113    1.135077    1.571239
N   -1.040925    1.373640    1.330473
C   -0.640632    2.301232    2.213065
C   -1.739157    2.718517    3.054137
C   -2.863478    1.992759    2.638005
C   -5.186191   -1.882270    0.131226
C   -4.220443    2.051042    3.188252
C   -5.614318   -1.595406    1.441925
C   -6.957536   -1.717295    1.795207
C   -7.903986   -2.121287    0.850781
C   -7.494604   -2.402210   -0.455188
C   -6.152235   -2.287415   -0.810985
```

```
C   -5.353320    1.895140    2.366693
C   -6.636881    1.958260    2.906311
C   -6.820495    2.176066    4.273224
C   -5.705805    2.328237    5.101465
C   -4.421175    2.267309    4.566285
C   -1.658634    3.749453    4.014441
C   -1.550866    4.656258    4.822078
C   -3.526848   -3.768393   -1.772183
C   -3.975262   -4.757526   -2.326355
C   -0.601158   -2.652528   -1.964239
C    0.738157    2.802443    2.315294
C   -0.393009   -4.043941   -1.976839
C    0.656332   -4.599020   -2.704473
C    1.529976   -3.797226   -3.452724
C    1.316597   -2.412121   -3.441443
C    0.275611   -1.846586   -2.710662
C    1.364949    2.878900    3.573005
C    2.672072    3.341430    3.686083
C    3.397689    3.758336    2.559911
C    2.762084    3.700392    1.312944
C    1.456280    3.230351    1.188176
C    2.684209   -4.402365   -4.219633
C    3.981708   -4.495319   -3.389749
C    5.150307   -5.103291   -4.175406
C    6.449236   -5.192530   -3.364211
C    7.619310   -5.802891   -4.146717
C    8.914309   -5.882713   -3.331885
C    4.832550    4.218809    2.688154
C    5.837990    3.048800    2.719676
C    7.296428    3.510372    2.828177
C    8.299033    2.349158    2.848825
C    9.760884    2.803949    2.947801
C   10.755069    1.638221    2.964340
C    1.946144    1.576954   -1.832083
C    2.208683    2.667101   -2.736278
C    0.956626    3.230745   -3.031982
C   -0.026723    2.445547   -2.325286
N    0.565131    1.475792   -1.607789
N    2.904253    0.840957   -1.287318
C    2.813827   -0.113299   -0.381268
N    1.653996   -0.550008    0.273914
C    1.991859   -1.603086    1.025934
C    3.404496   -1.891124    0.900606
C    3.933725   -0.933152    0.025652
C    3.520759    3.103510   -3.227126
C    5.327018   -0.788556   -0.406722
```

C	4.530201	2.176896	-3.550502
C	5.765701	2.609159	-4.028852
C	6.024904	3.971800	-4.190703
C	5.035084	4.903065	-3.868161
C	3.796512	4.474903	-3.394080
C	6.149136	-1.922755	-0.560835
C	7.481050	-1.794693	-0.950742
C	8.024599	-0.531674	-1.197429
C	7.220179	0.601123	-1.055509
C	5.887217	0.477679	-0.666059
C	4.079439	-2.877510	1.650078
C	4.621353	-3.729375	2.333698
C	0.652463	4.264092	-3.944017
C	0.350240	5.138806	-4.737462
C	-1.483904	2.613664	-2.414492
C	1.030734	-2.335096	1.860148
C	-2.073481	3.886726	-2.328800
C	-3.452543	4.038979	-2.455875
C	-4.289169	2.939574	-2.692558
C	-3.695750	1.672105	-2.780550
C	-2.321907	1.507522	-2.639886
C	0.107025	-1.656353	2.671698
C	-0.823391	-2.361427	3.430186
C	-0.872644	-3.761882	3.402242
C	0.063870	-4.435699	2.604638
C	1.005966	-3.741002	1.851255
C	-5.785907	3.100599	-2.845216
C	-6.589384	2.606001	-1.625121
C	-8.105969	2.719195	-1.825973
C	-8.919757	2.223327	-0.623802
C	-10.437344	2.308463	-0.833273
C	-11.241552	1.815523	0.374024
C	-1.938095	-4.517562	4.163748
C	-3.211036	-4.751064	3.322668
C	-4.321333	-5.478425	4.090528
C	-5.584345	-5.705520	3.249447
C	-6.715641	-6.403270	4.015304
C	-7.970176	-6.623854	3.163684
Zn	-0.107139	0.314162	-0.103580
H	-4.888670	-1.271939	2.177584
H	-7.263647	-1.487886	2.812228
H	-8.950546	-2.215298	1.128972
H	-8.223039	-2.708082	-1.201826
H	-5.846559	-2.499002	-1.829744
H	-5.219838	1.726645	1.305114
H	-7.495965	1.834819	2.252908

```
H   -7.823067   2.225744   4.690182
H   -5.834763   2.488033   6.168886
H   -3.561617   2.371798   5.219547
H   -1.049367  -4.688697  -1.403054
H    0.797399  -5.677665  -2.693643
H    1.969323  -1.764583  -4.022430
H    0.127961  -0.772719  -2.744290
H    0.827084   2.560027   4.459784
H    3.141121   3.376891   4.667139
H    3.292194   4.033912   0.423912
H    0.976309   3.229003   0.216718
H    2.409872  -5.407993  -4.565428
H    2.880140  -3.804913  -5.119898
H    4.254975  -3.492103  -3.035088
H    3.789240  -5.094900  -2.489073
H    4.869857  -6.107951  -4.525928
H    5.328812  -4.504894  -5.081292
H    6.728987  -4.186693  -3.018019
H    6.271306  -5.788384  -2.456508
H    7.340084  -6.809552  -4.489258
H    7.794883  -5.210676  -5.056167
H    9.729403  -6.325193  -3.916036
H    9.240545  -4.886189  -3.008462
H    8.779400  -6.494169  -2.431219
H    5.081430   4.883033   1.850345
H    4.949740   4.813684   3.604305
H    5.595366   2.388807   3.564130
H    5.710445   2.440183   1.814458
H    7.529789   4.177111   1.984408
H    7.421206   4.117561   3.737467
H    8.068454   1.684776   3.694819
H    8.167935   1.740496   1.942299
H    9.991192   3.469415   2.103298
H    9.892226   3.410167   3.855616
H   11.789676   1.993882   3.032997
H   10.573087   0.974648   3.818678
H   10.669468   1.032754   2.053548
H    4.338463   1.118324  -3.424649
H    6.527989   1.875242  -4.276231
H    6.989573   4.305438  -4.564124
H    5.227251   5.966987  -3.980715
H    3.036678   5.205647  -3.137434
H    5.734497  -2.909208  -0.384649
H    8.092722  -2.685933  -1.065559
H    9.063691  -0.431957  -1.500095
H    7.628057   1.589024  -1.251811
```

H	5.269104	1.360802	-0.564510
H	-1.448935	4.756136	-2.151873
H	-3.887633	5.032569	-2.373610
H	-4.316536	0.800826	-2.975736
H	-1.888722	0.519465	-2.744204
H	0.138995	-0.573631	2.728743
H	-1.523672	-1.813693	4.056705
H	0.047984	-5.522938	2.566714
H	1.709844	-4.284597	1.230099
H	-6.025057	4.155582	-3.031109
H	-6.120614	2.546062	-3.733213
H	-6.325510	1.559633	-1.418545
H	-6.286564	3.179709	-0.738231
H	-8.369972	3.766122	-2.037627
H	-8.395157	2.146655	-2.720004
H	-8.642211	1.182112	-0.401764
H	-8.644846	2.810302	0.265471
H	-10.715151	3.347990	-1.058585
H	-10.712999	1.721373	-1.720918
H	-12.320374	1.883532	0.192703
H	-11.007453	0.768805	0.604724
H	-11.016731	2.408966	1.269020
H	-1.543093	-5.487501	4.494346
H	-2.206220	-3.962075	5.072172
H	-3.586248	-3.783213	2.963627
H	-2.946119	-5.323669	2.423018
H	-3.943594	-6.446195	4.453555
H	-4.581480	-4.898122	4.988598
H	-5.945841	-4.739043	2.869645
H	-5.326271	-6.301500	2.361457
H	-6.356342	-7.370066	4.396360
H	-6.975328	-5.805799	4.901052
H	-8.765359	-7.112805	3.738379
H	-8.364706	-5.671575	2.788346
H	-7.751484	-7.255122	2.293470
C	-1.381226	5.714511	5.756266
C	-2.510309	6.286383	6.444445
C	-0.102540	6.204116	6.010597
C	-3.839569	5.845031	6.220404
C	-2.281871	7.342192	7.385413
C	0.105869	7.244910	6.937131
H	0.740255	5.770225	5.481342
C	-4.895659	6.414726	6.897822
H	-4.014129	5.052597	5.499404
C	-3.394084	7.905228	8.068171
C	-0.957551	7.801736	7.613233

```
H    1.115643    7.604724    7.114593
C   -4.672506    7.453251    7.832877
H   -5.907731    6.065997    6.710622
H   -3.214438    8.705566    8.782328
H   -0.797614    8.603470    8.330159
H   -5.513431    7.894199    8.361483
C   -4.548602   -5.904936   -2.940196
C   -3.871923   -6.595269   -4.008169
C   -5.787200   -6.366368   -2.501079
C   -2.612913   -6.173598   -4.507111
C   -4.495030   -7.747327   -4.588616
C   -6.388499   -7.499759   -3.083571
H   -6.288104   -5.838366   -1.695510
C   -1.993930   -6.858946   -5.529837
H   -2.142988   -5.298281   -4.069943
C   -3.827945   -8.430696   -5.641301
C   -5.758399   -8.178307   -4.103624
H   -7.355085   -7.835731   -2.718301
C   -2.605357   -7.999236   -6.103035
H   -1.030108   -6.520420   -5.900456
H   -4.305448   -9.304865   -6.077895
H   -6.220384   -9.054395   -4.552355
H   -2.107587   -8.531239   -6.909368
C    5.212533   -4.736417    3.144579
C    6.643517   -4.884335    3.221553
C    4.393744   -5.594344    3.874824
C    7.534133   -4.032720    2.519159
C    7.185969   -5.925803    4.042186
C    4.942270   -6.611913    4.680208
H    3.317010   -5.468228    3.816347
C    8.897965   -4.204379    2.615576
H    7.123762   -3.234989    1.908066
C    8.597388   -6.076225    4.116129
C    6.307425   -6.778845    4.761461
H    4.277129   -7.266047    5.237222
C    9.436596   -5.237380    3.418946
H    9.565194   -3.539596    2.073566
H    9.003349   -6.869651    4.739407
H    6.731817   -7.565546    5.380585
H   10.513889   -5.363365    3.486254
C   -0.046923    6.153327   -5.651152
C    0.915293    6.805013   -6.502471
C   -1.387727    6.522616   -5.722825
C    2.292250    6.464967   -6.491618
C    0.463382    7.829830   -7.395694
C   -1.817469    7.530644   -6.608436
```

```
H   -2.105673   6.018655   -5.083125
C    3.184706   7.110078   -7.319898
H    2.633088   5.680717   -5.823057
C    1.411748   8.476494   -8.233913
C   -0.914095   8.174072   -7.425682
H   -2.870328   7.797193   -6.640367
C    2.742559   8.127688   -8.198321
H    4.235425   6.833366   -7.300550
H    1.063134   9.254772   -8.908878
H   -1.244181   8.953885   -8.107785
H    3.456109   8.629873   -8.846138
```

References

[1] Z. Otwinowski, W. Minor, In *Macromolecular Crystallography, Pt A;* C. W. Carter, Jr., R. M. Sweet, Eds., Methods in Enzymology, Vol. 276; **1997**; pp 307–326.

[2] G. M. Sheldrick, *Acta Crystallography, Sect. A: Found. Crystallography,* **2008,** *64,* 112–122. doi:10.1107/S0108767307043930

[3] G. M. U. o. G. *Sheldrick;* Germany, http://shelx.uni-ac.gwdg.de/SHELX/.

[4] C. B. Hübschle, G. M. Sheldrick, B. *J.* Dittrich, *Appl. Crystallography,* **2011,** *44,* 1281–1284. doi:10.1107/S0021889811043202.

[5] Gaussian 16, Revision A.03, M. J. Frisch, G. W. Trucks, H. B. Schlegel, G. E. Scuseria, M. A. Robb, J. R. Cheeseman, G. Scalmani, V. Barone, G. A. Petersson, H. Nakatsuji, X. Li, M. Caricato, A. V. Marenich, J. Bloino, B. G. Janesko, R. Gomperts, B. Mennucci, H. P. Hratchian, J. V. Ortiz, A. F. Izmaylov, J. L. Sonnenberg, D. Williams-Young, F. Ding, F. Lipparini, F. Egidi, J. Goings, B. Peng, A. Petrone, T. Henderson, D. Ranasinghe, V. G. Zakrzewski, J. Gao, N. Rega, G. Zheng, W. Liang, M. Hada, M. Ehara, K. Toyota, R. Fukuda, J. Hasegawa, M. Ishida, T. Nakajima, Y. Honda, O. Kitao, H. Nakai, T. Vreven, K. Throssell, J. A. Montgomery, Jr., J. E. Peralta, F. Ogliaro, M. J. Bearpark, J. J. Heyd, E. N. Brothers, K. N. Kudin, V. N. Staroverov, T. A. Keith, R. Kobayashi, J. Normand, K. Raghavachari, A. P. Rendell, J. C. Burant, S. S. Iyengar, J. Tomasi,

M. Cossi, J. M. Millam, M. Klene, C. Adamo, R. Cammi, J. W. Ochterski, R. L. Martin, K. Morokuma, O. Farkas, J. B. Foresman, and D. J. Fox, Gaussian, Inc., Wallingford CT, 2016.

[6] Hehre, W. J.; Radon, L.; v. R. Schleyer, P.; Pople, J. A. *Ab Initio Molecular Orbital Theory;* Wiley-Interscience: New York, 1986.

[7] P. J. Stephens, F. J. Devlin, C. F. Chabalowski, M. J. Frisch, *J. Phys. Chem.* **1994**, *98*, 11623–11627.

[8] A. D. Becke, *J. Chem. Phys.* 1993, *98*, 5648–5652.

[9] C. Lee, W. Yang, R. G. Parr, *Phys. Rev. B* 1988, *37*, 785–789.

[10] S. H. Vosko, L. Wilk, M. Nusair, *Can. J. Phys.* 1980, *58*, 1200–1211.

[11] N. Godbout, D. R. Salahub, J. Andzelm, E. Wimmer *Can. J. Chem.* 1992, *70*, 560–571

[12] S. Miertus, E. Scrocco, J. Tomasi, *Chem. Phys.* 1981, *55*, 117–129.

[13] J. Tomasi, B. Mennucci, R. Cammi, *Chem. Rev.* 2005, *105*, 2999–3093.

[14] E. Cancès, B Mennucci, J. Tomasi, *J. Chem. Phys.* 1997, *107*, 3032–3041.

[15] B. Mennucci, E. Cancès, J. Tomasi, *J. Phys. Chem. B* 1997, *101*, 10506–10517.

[16] S. I. Gorelsky, AOMix: Program for Molecular Orbital Analysis; University of Ottawa, version 6.94, 2018, http://www.sg-chem.net.

[17] S. I. Gorelsky, A. B. P. Lever, *J. Organomet. Chem.* 2001, *635*, 187–196.

[18] F. S. Etheridge, R. J. Fernando, S. Pejic, M. Zeller and G. Sauve, *Beilstein J. Org. Chem.,* **2016**, *12*, 1925–1938.

[19] Z. Li, J. D. A. Lin, H. Phan, A. Sharenko, C. M. Proctor, P. Zalar, Z. Chen, A. Facchetti and T.-Q. Nguyen, *Adv. Funct. Mater.* **2014**, *24*, 6989–6998.

[20] R. Po, G. Bianchi, C. Carbonera, A. Pellegrino, *Macromolecules*, **2015**, *48*, 453.

[21] J. Min, Y. N. Luponosov, C. Cui, B. Kan, H. Chen, X. Wan, Y. Chen, S. A. Ponomarenko, Y. Li and C. J. Brabec, *Adv. Energy Mater.*, **2017**, *7*, 1700465.

[22] X. Li, F. Pan, C. Sun, M. Zhang, Z. Wang, J. Du, J. Wang, M. Xiao, L. Xue, Z. Zhang, C. Zhang, F. Liu, Y. Li, *Nat. Commun.*, **2019**, *10*, 519

[23] C. Sun, F. Pan, H. Bin, J. Zhang, L. Xue, B. Qiu, Z. Wei, Z. Zhang, Y. Li, *Nat. Commun.*, **2018**, *9*, 743.

[24] M, Zhang , X. Guo , W. Ma , H. Ade , and J. Hou, *Adv. Mater.,* **2014**, *26*, 5880-5885.